Specificities and commonalities of carbapenemase producing *Escherichia coli* isolated in France from 2012 to 2015.

[1,2]Rafael Patiño-Navarrete[#], [1,2]Isabelle Rosinski-Chupin[#], [1,2]Nicolas Cabanel, [1,2,3]Pengdbamba Dieudonné Zongo, [1,4]Mélanie Héry, [1,4]Saoussen Oueslati, [1,4]Delphine Girlich, [1,4,5,6]Laurent Dortet, [1,4,6]Rémy A Bonnin, [1,4,5,6]Thierry Naas[$] and [1,2,*]Philippe Glaser[$].

[$ and #] Contributed equally

[1]Unité EERA, Institut Pasteur, APHP, Université Paris Saclay, [2]UMR3525, CNRS, Université de Paris 28 rue du Dr Roux, 75015, Paris, France; [3]Sorbonne Université, Paris, France, [4] Team "Resist" INSERM U1184 "Immunology of Viral, Auto-Immune, Hematological and Bacterial diseases (IMVA-HB),"; [5]Department of Bacteriology-Hygiene, Bicêtre Hospital, APHP, [6]Associated French National Reference Center for Antibiotic Resistance, Le Kremlin-Bicêtre, France.

*Corresponding author:

Philippe GLASER,

Institut Pasteur, 28 Rue du Dr Roux, 75724 Paris Cedex 15,

Tel + 33 1 45 68 89 96 - E-mail: pglaser@pasteur.fr

Running title: Carbapenemase producing *E. coli* from the French NRC

ABSTRACT

Carbapenemase-producing *Escherichia coli* (CP-*Ec*) represent a major public health threat with a risk of dissemination in the community as it has occurred for lineages producing extended spectrum ß-lactamases. To characterize the extend of CP-*Ec* spread in France, isolates from screening and infection samples received at the French National Reference Centre laboratory (F-NRC) for carbapenemase-producing Enterobacterales were investigated. Six hundred and ninety one CP-*Ec* isolates collected between 2012 and 2015 and 22 before were fully sequenced. Analysis of their genome sequences revealed some disseminating multidrug resistant (MDR) lineages frequently acquiring diverse carbapenemase genes mainly belonging to clonal complex (CC) 23 (ST 410) and CC10 (ST10, ST167) and sporadic isolates including rare ST131 isolates (n=17). However, the most represented ST was ST38 (n=92) with four disseminated lineages carrying $bla_{\text{OXA-48-like}}$ genes inserted in the chromosome. Globally, the most frequent carbapenemase gene (n=457) was $bla_{\text{OXA-48}}$. It was also less frequently associated with MDR isolates being the only resistance gene in 119 isolates. Thus, outside the ST38 clades, its acquisition was frequently sporadic with no sign of dissemination, reflecting the circulation of the IncL plasmid pOXA-48 in France and its high frequency of conjugation. In contrast $bla_{\text{OXA-181}}$ or bla_{NDM} genes were often associated with the evolution of MDR *E. coli* lineages characterized by mutations in *ftsI* and *ompC.*

IMPORTANCE

Carbapenemase-producing *Escherichia coli* (CP-*Ec*) might be difficult to detect, as minimal inhibitory concentrations can be very low. However, their absolute number and their proportion among carbapenem-resistant *Enterobacterales* have been increasing, as reported by WHO and national surveillance programs. This suggests a still largely uncharacterized community spread of these isolates. Here we have characterized the diversity and evolution of CP-*Ec* isolated in France before 2016. We show that carbapenemase genes are associated with a wide variety of *E. coli* genomic backgrounds and a small number of dominant phylogenetic lineages. In a significant proportion of CP-*Ec*, the most frequent carbapenemase gene $bla_{\text{OXA-48}}$, was detected in isolates lacking any other resistance gene, reflecting the dissemination of pOXA-48 plasmids, likely in the absence of any antibiotic pressure. In contrast carbapenemase gene transfer may also occur in multi-drug resistant *E. coli*, ultimately giving rise to at-risk lineages encoding carbapenemases with a high potential of dissemination.

54 **INTRODUCTION**

55 *Escherichia coli* is one of the first causes of diverse bacterial infections in the community and in the
56 hospital. In particular, it is the most frequent cause of urinary tract infection (UTI) and 50-60% of
57 women will suffer at least once a UTI during her life (1). Therefore, multidrug resistance (MDR) in *E. coli*
58 is a major public health issue making *E. coli* infections more difficult to treat. In addition, as
59 carbapenemase-producing *Enterobacterales* (CPE) are increasingly detected (2, 3) and *E. coli* is a
60 ubiquitous member of the human gut microbiome, carbapenemase-producing *E. coli* (CP-*Ec*) are also
61 becoming a major actor for the global dissemination of carbapenemase genes (4).

62 The emergence and spread of carbapenem-resistant Gram-negative bacteria is mainly linked to the
63 widespread dissemination through horizontal gene transfer (HGT) of mobile genetic elements (MGEs)
64 encoding carbapenemases. These carbapenemases belong to Ambler class A (mainly KPC-type), class
65 B (metallo-β-lactamases IMP-, VIM- and NDM-types) or class D (OXA-48-like enzymes) of beta-
66 lactamases (5). The global epidemiology of extended spectrum ß-lactamases (ESBL) producing *E. coli*
67 has been characterized through multiple studies, revealing in Western countries the major
68 contribution of the sequence type (ST)131 lineage in the high prevalence of $bla_{\text{CTX-M}}$ family ESBL genes
69 (6). Much less is known with respect to CP-*Ec*.

70 Since in 2012, the French National Reference Centre Laboratory for carbapenemase-producing
71 *Enterobacterales* (F-NRC) has experienced a steady increase in the number of CP-*Ec* isolates received
72 each year (2). A multi locus sequence typing (MLST) analysis of isolates received in 2012 and 2013
73 revealed a broad diversity of STs, as the 140 analyzed isolates belonged to 50 different STs. However,
74 a few STs were over-represented (7), such as the ST38 (24 isolates) and the ST410 (10 isolates). In that
75 study, only one isolate belonged to ST131, contrasting with the situation in the UK where ST131
76 isolates represented 10% of the CP-*Ec* isolates received between 2014 and 2016 by Public Health
77 England (8). On the other hand, a genome based survey of CPE in the Netherlands between 2014 and
78 2018, revealed that the 264 analyzed *E. coli* isolates belonged to 87 different STs, with three dominant
79 lineages, ST38 (n=46), ST167 (n=22) and ST405 (n=16) representing 32 % of the isolates (9). F-NRC
80 isolates also showed a predominance of isolates producing OXA-48-like carbapenemases followed by
81 NDM-producing isolates and suggested clonally related isolates among ST38 OXA-48-producing
82 isolates and ST410 OXA-181-producing isolates, respectively (7).

83 Whole-genome sequencing (WGS) significantly increases our ability to infer phylogenetic relationships
84 between isolates. By sequencing 50 ST410 CP-*Ec* isolates received by the F-NRC between 2011 and
85 2015 (10) we showed that 36 (72%) belonged to a newly described ST410 lineage producing OXA-181
86 (11). We showed that this clade is characterized by mutations in the two porin genes *ompC* and *ompF*
87 leading to a decreased outer membrane permeability to certain ß-lactams and by a four-codon
88 duplication (YRIN) in the *ftsI* gene encoding the penicillin binding protein 3 (PBP3) leading to a

89 decreased susceptibility to ß-lactams targeting this PBP (10). After a thorough analysis of CP-*Ec*
90 genome sequences from public databases for mutations in these three genes, we proposed that CP-*Ec*
91 followed three different evolutionary trajectories. In some lineages which are enriched in CP-*Ec*
92 isolates and have disseminated globally, acquisition of carbapenem resistance genes might have been
93 facilitated by the mutations in porin genes and in *ftsI*. In ST38, the genetic background and in particular
94 a specific *ompC* allele with reduced permeability to some ß-lactams may have similarly facilitated the
95 acquisition of carbapenemase genes. In contrast, other CP-*Ec* isolates including from ST131 might have
96 occurred sporadically following the acquisition of plasmids encoding carbapenemase and with no clue
97 of dissemination (10).
98 Here we thoroughly characterized the diversity of CP-*Ec* circulating in France by sequencing the
99 genome of almost all isolates received by the F-NRC from its creation in 2012 until 2015 (Table S1). By
100 combining whole genome phylogeny with the addition of *E. coli* genome sequences publicly available
101 (Table S2), and tracking mutations in candidate genes, we show that three different situations are
102 encountered. The high transmission potency of the IncL pOXA-48 plasmids has led to a high frequency
103 of OXA-48-producing isolates, often characterized by susceptibility to most non-ß-lactam antibiotics.
104 On the other hand, an increasing number of CP-*Ec* lineages, mainly producing OXA-181 and NDM
105 carbapenemases, are observed in France as in other European countries. These lineages are multi-drug
106 (MDR) or extensively drug resistant (XRD) lineages, they show several mutations in quinolone
107 resistance determining regions (QRDR) and are often mutated in *ftsI* and in porin genes. Finally, the
108 rapid dissemination of four OXA-48/OXA-244 ST38 lineages might have been favored by the
109 chromosomal integration of the carbapenemase gene.
110
111 **RESULTS**
112
113 **CP-*Ec* isolates collected until 2015 by the French National Reference Center**.
114 Isolates analyzed in this work were sent to the F-NRC laboratory on a voluntary basis from private and
115 public clinical laboratories from different parts of France mainly between the years 2012 to 2015.
116 During this period, we encountered a regular increase in the number of isolates received each year
117 (Fig 1A) corresponding to an increasing number of isolated strains and an increasing frequency of
118 isolates sent to the F-NRC. 713 CP-*Ec* isolates, including 22 collected from 2001 to 2011 were submitted
119 to WGS. The 691 sequenced isolates of the 2012-2015 period represented 87.5 % of the 790 CP-*Ec*
120 isolates received by the F-NRC during this period.
121 The majority of the sequenced isolates (66.5%, 474/713) were from rectal swab screening of patients
122 suspected of carrying CPE (patients repatriated from an hospital abroad, patients that have visited a
123 foreign country within the last six months, contact patients of a former carrier, or a previously known

124 carrier), 24% (172/713) were considered to be responsible for infection (isolated from clinical
125 samples), and the source was unknown for 67 isolates (Fig. 1A, Table S1). During the four-year period,
126 The number of infection-related isolates was found to increase more slowly than the number of
127 screening or of unknown source isolates. A nearly two-fold decrease in the proportion of clinical versus
128 total isolates was observed between 2013 and 2014 (Fig. 1B). Among the 172 isolates associated with
129 disease, 122 were isolated from urine (71%), 15 from blood samples, eight from deep site samples,
130 eight from wound samples, nine from the respiratory tract, three from vaginal samples, three from
131 pus, three from bile, and one from the skin of a newborn. All these isolates were previously identified
132 as carbapenemase producers by PCR.
133
134 **Diversity of CP-*Ec* isolates as assessed by whole genome sequencing.**
135 The genome sequences of the 713 CP-*Ec* isolates were first analyzed following *de novo* assembly. For
136 each isolate, we determined its MLST type (Achtman scheme), its phylogroup (ClermonTyping) and its
137 antibiotic resistance genes (ARG) content. We also searched for mutations in the QRDRs of *gyrA*, *parC*
138 and *parE,* and for mutations in *ftsI*, *ompC* and *ompF* we previously identified as associated with CP-*Ec*
139 disseminated lineages (10) (table S1). F-NRC CP-*Ec* were assigned to 168 different STs including six new
140 allelic combinations. ST38 was the most prevalent ST (n=92, 12.9 %), followed by ST10 (n=67, 9.4 %),
141 ST410 (n=64, 9 %), and ST167 (n=34, 4.8 %). Ten additional STs were represented by at least 10 isolates
142 (Fig. S1A, table S1) and 154 STs with less than ten isolates including 102 STs with a single isolate.
143 We next performed a core genome phylogeny following read mapping using strain MG1655
144 (NC_000913.3) as reference genome sequence. The phylogenetic tree, estimated from 372,238 core
145 SNPs was consistent with the results of phylogroup determination by using *in silico* ClermonTyping (12)
146 except for a few isolates (Fig. 2). In agreement with the MLST-based analysis, this tree showed a broad
147 diversity of CP-*Ec* isolates belonging to the eight phylogroups and three dominant clades
148 corresponding to CC10 (phylogroup A; including ST10, ST167 and ST617), CC23 (phylogroup C;
149 including ST410, ST88 and ST90) and ST38 (phylogroup D) with 161, 97, and 98 isolates respectively,
150 accounting for 49.9 % of the F-NRC CP-*Ec* isolates analyzed (Fig. 2). Phylogroup B2 isolates represented
151 11 % of the total isolates (n=80) and only 17 CP-ST131 isoaltes were identified. Fluctuations in the
152 proportions of the main STs could be observed during the four years of the analysis but no clear
153 tendency could be identified (Fig. S1A).
154 Infection-related and screening isolates were intermixed throughout the phylogeny (Fig. 2). However,
155 an enrichment in infection-related isolates was observed in phylogroup C (Pearson's Chi-squared test,
156 $p<0.02$, ddl1) and phylogroup B2 (Pearson's Chi-squared test $p<0.0005$, ddl1) (Fig. S1B). In phylogroup

157 B2, 5 out of 9 ST127 isolates, 5 out of 17 ST131 isolates and 7 out of 8 ST636 were responsible for UTIs
158 (Table S1).
159
160 **Diversity of antibiotic resistance genes carried by CP-*Ec* isolates**
161 The number of acquired ARGs was found to vary between 1 and 26 among the 713 CP-*Ec* isolates. The
162 median was higher in phylogroup C isolates (m=16) and lower in isolates from phylogroup B2 (m=3)
163 compared to other phylogroups (Medians: A: 9; B1: 9; D: 11) (Fig. 3A). An ESBL of the CTX-M family
164 was present in 40.7% (N=290) of the isolates, with a predominance of $bla_{\text{CTX-M-15}}$ gene (N=205) (Table
165 S1). Mutations in g*yrA*, *parC* and/or *parE* potentially leading to fluoroquinolone (FQ) resistance
166 occurred in 425 CP-*Ec* isolates (59.6%), with mutations in *gyrA*, *parC* and *parE* identified in 412 isolates,
167 309 and 261 isolates respectively (Table S1). Up to five mutations in QRDRs were identified in 19
168 isolates and 250 isolates had four mutations in QRDR, suggesting they have been submitted to a long-
169 term evolution under antibiotic pressure including FQ (Table S1). Globally a higher number of
170 mutations in QRDR was associated with a higher number of resistance genes (Fig. 3B), furthering the
171 link between the number of QRDR mutations and a likely evolution under antibiotic selective pressure
172 for CP-*Ec* isolates.
173 Four isolates from 2015, two ST648 collected in a same hospital at one-week interval, one ST216 and
174 one ST744, encoded a *mcr-9* gene conferring resistance to colistin (Table S1). Although not associated
175 with infection, the four isolates were MDR, carrying 13 to 20 acquired ARGs in addition to *mcr-9* and
176 carbapenemase genes ($bla_{\text{VIM-1}}$ for three of them, $bla_{\text{NDM-1}}$ and $bla_{\text{OXA-48}}$ for one). Determination of the
177 MIC for colistin for these four isolates were at the resistance breakpoint (MIC=2 mg/l).
178
179 **Diversity of carbapenemase genes**
180 Carbapenemase genes identified by WGS (Table S1) were in agreement with molecular data collected
181 by the F-NRC laboratory. The $bla_{\text{OXA-48}}$ and $bla_{\text{OXA-181}}$ genes were the most frequent carbapenemase
182 genes detected in 464 (65%) and 101 (14.1%) *E. coli* isolates respectively. Twenty-nine other isolates
183 carried minor $bla_{\text{OXA-48-like}}$ genes (Table S1). bla_{NDM} family genes were detected in 14.9% (106/713) of
184 the CP-*Ec* isolates ($bla_{\text{NDM-5}}$ in 49 isolates and $bla_{\text{NDM-1}}$ in 41). Three additional bla_{NDM} alleles were
185 identified: $bla_{\text{NDM-7}}$ (n=10) including a variant coding for a NDM7-like carbapenemase with a S24G
186 mutation, $bla_{\text{NDM-4}}$ (n=5), and $bla_{\text{NDM-6}}$ (n=1). Four different bla_{VIM} alleles were detected in 18 isolates:
187 $bla_{\text{VIM-1}}$ (n=8), $bla_{\text{VIM-4}}$ (n=8), $bla_{\text{VIM-2}}$ (n=1), and $bla_{\text{VIM-29}}$ (n=1). Only five *E. coli* isolates expressed $bla_{\text{KPC-}}$
188 $_{2}$ (n=2) or $bla_{\text{KPC-3}}$ (n=3) alleles. In twelve isolates, two different carbapenemase genes were found;
189 $bla_{\text{OXA-48}}$ / $bla_{\text{NDM-1}}$ was the most frequent co-occurrence (n=5) (Table S1).
190 The analysis of the number of additional ARGs and of mutations in QRDR regions showed that,
191 compared with other carbapenemase genes the presence of $bla_{\text{OXA-48}}$ was frequently associated with

192 less resistant isolates (Fig. 4A, 4B). In particular it was the only ARG in 117 isolates among the 457
193 (24.5%) encoding this carbapenemase, including 23 infection-related isolates. Among those isolates,
194 only five showed mutations in QRDR. Conversely, only two bla_{NDM-1} gene carrying isolates among 42
195 and one bla_{NDM-5} gene carrying isolates among 49 carried no other ARG.
196 A temporal analysis of the proportion of isolates displaying bla_{OXA-48} did not reveal significant variations
197 (Pearson's Chi-squared test, p=0.05, ddl= 3) during the 2012-2015 period (Fig. 4C). In contrast, the
198 frequency of $bla_{OXA-181}$ relatively to other alleles was found to significantly increase from 0 % in 2012
199 to 18.9% in 2015 (Pearson's Chi-squared test, $p < 0.0002$ ddl=3) (Fig. 4C).
200 We observed some association between the carbapenemase gene and the ST. Among the 22 STs with
201 at least seven F-NRC CP-*Ec* isolates, fourteen predominantly displayed bla_{OXA-48} (Fig. 5A); bla_{OXA-48} was
202 also predominant in STs represented by six or less isolates. In three lineages, ST410, ST940, and
203 ST1284, $bla_{OXA-181}$ was the predominant allele. These three STs grouped 74% of the $bla_{OXA-181}$ gene
204 carrying *E. coli* isolates from the F-NRC, and ST410 accounted for 50.5% of them. Finally, $bla_{OXA-204}$ was
205 the most prevalent allele in ST90 and bla_{NDM-5} the predominant allele in ST636.
206
207 **Characteristics of the STs preferentially associated with F-NRC CP-*Ec* isolates.**
208 Eight among the 14 STs with more than 10 CP-*Ec* isolates (ST410, ST167, ST940, ST405, ST617, ST90,
209 ST1284, ST101) were characterized by a larger number of ARGs (median ≥ 10) and a larger number of
210 mutations in QRDR as compared to ST38, ST10, ST131, ST69, ST88 and ST represented by less than
211 seven isolates (Fig. 5 B, C). ST648 isolates have an intermediate position, being highly mutated in QRDR
212 but less rich in ARGs. Analysis of CP-*Ec* isolates from the F-NRC for polymorphisms in *ftsI* revealed that
213 131 (18.4%) had a four-AA-insertion between positions 333 and 334 of PBP3, the insertion being
214 particularly prevalent in ST101, ST167, ST410 and ST1284 (Sup. Table 1 and Fig. 5D). Similarly, *ompC*
215 alleles we previously characterized as modifying susceptibility to antibiotics were more prevalent in
216 some STs: an ST38-like *ompC* allele resulting from a recombination event or a G138D mutation were
217 present in 33 and 26 isolates belonging to six different ST, whereas the R195L mutation was observed
218 in 50 isolates all from ST410 (Table S1 and Fig. 5E). In addition, 144 isolates belonging to phylogroups
219 D and F possessed the ST38-like allele inherited vertically. On the other hand the *ompF* gene was
220 pseudogeneized in 47 isolates (Table S1).
221 To analyze the phylogenetic relationships between F-NRC Cp-*Ec* and other Cp-*Ec* isolates collected
222 worldwide, we built ST-based maximum-likelihood trees for the 14 STs with more than 10 isolates and
223 included to this analysis genome sequences publicly available (Table S2). Together with the analysis of
224 QRDR mutations and mutations in *ftsI* and *ompC*, this showed that 51 (80%) of the ST410 (Fig.S2A), 17
225 (49%) of the ST167 (Sup Fig.S2B), 3 (33%) of the ST405 (Sup Fig.S2C) and 8 (62%) of the ST101 (Fig.
226 S2D) F-NRC CP-*Ec* belonged to internationally disseminating MDR subclades enriched in CP we

227 previously identified (10). Subclades characterized by mutations in *ftsI* and *ompC,* mainly expressed
228 $bla_{OXA-181}$ (ST410) or bla_{NDM} (other lineages). Other isolates belonging to these ST were dispersed on
229 their respective phylogenies and with no sign of clonal dissemination for most of them.
230 ST38 corresponded to the most represented ST (n=92) among the studied CP-*Ec*. The phylogenetic
231 reconstruction together with 314 additional non redundant CP-*Ec* genome sequences retrieved from
232 Enterobase (http://enterobase.warwick.ac.uk/) and 150 non-CP isolates from NCBI provided
233 evidence that 80.4% (n=67) of the French isolates clustered into four clades (Fig. 6). Three of them, G1
234 (n=35), G2 (n=25) and G4 (n=4) only contained isolates encoding bla_{OXA-48}, while G3 (n=7), included
235 isolates expressing bla_{OXA-48} or its single nucleotide derivative $bla_{OXA-244.}$ All but one isolates in G1
236 expressed $bla_{CTX-M-24}$, while isolates of G3 expressed $bla_{CTX-M-14b}$. The phylogenetic analysis provided
237 evidence of worldwide dissemination of G1, G3 and G4 clades and multiple introduction in France.
238 Strickingly, among the 28 isolates of the G2 clade, 24 were collected in France and four in the
239 Netherlands, suggesting at this time a more regional dissemination. In none of the isolates of the four
240 clades, an IncL plasmid, that generally encode bla_{OXA-48} (13), could be identified by PlasmidFinder (14).
241 It suggests a chromosomal integration as previously shown among ST38 isolates collected in the UK
242 (15). Analysis of representative isolates of the G1 and G3 cluster (G1: GCA_005886035.1; G3:
243 GCA_004759025.1), whose genome sequences were completely assembled, confirmed that bla_{OXA-48}
244 and $bla_{OXA-244}$, in these two isolates respectively, were chromosomally integrated. To assess the genetic
245 support of bla_{OXA-48} in the two other clades, we have determined the complete genome sequence of
246 two isolates belonging to G2 (CNR65D6) and G4 (G4:CNR85I8) by combining long-read Pacbio and
247 Illumina sequencing and found that both possess a chromosomally inserted bla_{OXA-48} gene. pOXA-48
248 plasmid sequences of various lengths were cointegrated with $bla_{OXA-48,}$ the whole sequence being
249 surrounded by IS*1* insertion sequences with different insertion sites for the four clades (Fig. 7). BLASTN
250 analyses on the assembled Illumina sequences of other isolates of each clade showed that isolates of
251 the same clade share the same insertion sites (see material and methods). A fifth clade, composed of
252 seven closely related French isolates corresponded to a possible outbreak in the East of Paris between
253 December 2014 and December 2015. These isolates are predicted to be highly resistant as they are
254 carrying in addition to $bla_{VIM-4,}$ $bla_{CTX-M-15}$, as well as 15 to 18 additional ARGs and five mutations in
255 QRDRs.
256 ST10 *E. coli* isolates are commensals of a variety of mammals and bird species (16) and studies in
257 different contexts have shown that this ST is also associated with ARGs carriage (17, 18). The 67 F-NRC
258 ST10 CP-*Ec* isolates were distributed throughout the ST10 phylogeny. Nonetheless 31 isolates
259 belonged to a clade enriched with carbapenemase producers (Fig. S3A, in green) that mainly expressed
260 bla_{OXA-48}, with the exception of three isolates expressing $bla_{OXA-181}$, three expressing bla_{NDM-5} and one
261 and bla_{VIM-4}. Two of the $bla_{OXA-181}$ and the three bla_{NDM-5} expressing isolates were closely related, shared

262 a CTX-M-27 ESBL, four mutations in QRDR and a *ftsI* allele with a four AA YRIN insertion (Fig. S3A, in
263 red).
264 ST131 isolates are major contributors for extra-intestinal infections and the main responsible for the
265 dissemination of CTX-M-15 ESBL (19, 20). ST131 evolution has been thoroughly analyzed and four main
266 lineages A, B, C1 and C2 have been described (21). We identified only 17 ST131 CP-*Ec* isolates received
267 by the F-NRC (Fig. 2), ten belonged to lineage A, while the others were scattered in the three other
268 lineages (Fig. S3B). The main carbapenemase associated with these isolates was OXA-48 (N=10). We
269 also did not observe any association with the carriage of $bla_{\text{CTX-M}}$ genes, as only four ST131 CP-*Ec*
270 isolates carryied a $bla_{\text{CTX-M-15}}$ gene. These results are in accordance with the UK survey (8) and our
271 previous observations from sequences retrieved from public databases (10).
272 ST940 (phylogroup B1) and ST1284 (phylogroup A) represented 2.4% (n=17) and 1.9% (n=14) of the
273 sequenced isolates while they were poorly represented in sequence databases. For instance, in May,
274 2021, only 83 and 103 sequences genome sequences could be retrieved from Enterobase for these ST
275 respectively, but with 43% (n=36) and 22% (n=22) carrying a carbapenemase gene respectively. This
276 suggested that ST940 and ST1284 were associated with the dissemination of carbapenemase genes.
277 Phylogenetic trees were drawn by adding the non-redundant sequences from enterobase to those of
278 the F-NRC and NCBI. For ST940 (Fig. S4A) this revealed a well-differentiated sub-clade of 18 isolates
279 from Asia, Australia and Europe carrrying $bla_{\text{NDM-5}}$ and sharing mutations in *ftsI* and *ompC*. Isolates
280 from the F-NRC were distributed on the tree, showing that the over-representation of ST940 in France
281 did not result from local outbreaks. Three F-NRC isolates belonged to a second smaller sub-clade of
282 bla_{NDM} expressing isolates, also mutated in *ftsI* and o*mpC*. In contrast, in ST1284, thirteen encoding
283 $bla_{\text{OXA-181}}$, were found to be closely related (Fig. S4B). Metadata analysis showed that 12 out of them
284 were recovered from the same health facility in the Paris suburb during a one-month period in 2015,
285 demonstrating a local outbreak origin. A fourteenth unrelated isolate expressed $bla_{\text{NDM-5}}$. The F-NRC
286 isolates belonged to a clade characterized by four mutations in QRDR determinants, a YRIN duplication
287 in PBP3, a G137D mutation in OmpC and containing additional OXA-181- or NDM-producing isolates.
288 Among the fifteen ST90 CP-*Ec* isolates, nine encoding the $bla_{\text{OXA-204}}$ allele were isolated in hospitals East
289 of Paris between August 2012 to April 2013 and suspected to be associated with the use of a
290 contaminated endoscope (22). Isolates closely related to this outbreak reappeared in 2014 (three
291 times), and in 2015 (twice), also in East of Paris located hospitals. They belonged to a MDR clade
292 characterized by four mutations in QRDR (Fig. S5A). Finally, in the four last STs with more than 10 CP-
293 *Ec* isolates (ST69, ST88, ST617, and ST648), French CP-*Ec* isolates were distributed throughout their
294 respective phylogenetic trees (FigS5B and C,S6A and B) with no sign of clonal dissemination, except for
295 a small cluster of five ST69 from two geographical regions and expressing *bla*OXA-48.

296 In addition to potential outbreaks detected in ST38 (bla_{VIM-4}), in ST90 ($bla_{OXA-204}$) and ST1284 ($bla_{OXA-181}$), we also found evidence for another potential outbreak among isolates belonging to the ST359. The five isolates encoded bla_{OXA-48} and $bla_{CTX-M-32}$ and had three mutations in QRDR. They were isolated during January 2014, four of them in the south-eastern part of France and one in the Parisian suburbs.

DISCUSSION

The prevalence of CP-*Ec* is increasing worldwide. However whether this reveals conjugation event in *E. coli* isolates by circulating CP-encoding plasmids or the emergence and dissemination of at-risk clones is still largely unknown. Here, we have analyzed, by using WGS, 691 (87.8%) of the CP-*Ec* isolates received by the F-NRC during the period 2012-2015 and 22 isolates from the Bicêtre hospital strain collection (2001-2011) to characterize both the diversity of carbapenemase genes and of CP-*Ec* isolates in France. Altogether 713 CP-*Ec* were sequenced, representing to our knowledge the most extended collection of CP-*Ec* sequenced, published to date.

The number of CP-*Ec* isolates sent to the F-NRC was found to strongly increase during the four-year period of analysis, which might be a consequence of an increased circulation of CP-*Ec* in France but also of an increased screening of potential CPE carriers at their admission at hospital. Indeed, while the number of infection-related CP-*Ec* isolates was regularly increasing, their proportion compared to the total number of received and sequenced isolates decreased by two-fold, with a clear change observed between 2013 and 2014 (Fig. 1). This is likely a consequence of the implementation of the recommendations on MDR screening of the French Public Health Advisory Board 2013 (23). However, as CP-*Ec* isolates were sent on a voluntary basis by clinical laboratories, we cannot exclude some sampling bias.

The most predominant carbapenemase allele was bla_{OXA-48} (65%) followed by $bla_{OXA-181}$ (14.1%) which detection constantly increased from no cases in 2012 to 73 in 2015. Next was bla_{NDM-5} that was found to progressively substitute to the bla_{NDM-1} gene in frequency of detection (Fig. 4). The predominance of $bla_{OXA-48-like}$ genes and particularly of bla_{OXA-48}, among CP-*Ec* was also noted in other studies (9, 24,25) although in lower proportions. The small number of bla_{KPC} genes detected in these studies is in contrast with the situation reported in *K. pneumoniae* for many European countries (26). However, bla_{OXA-48} was found the most prevalent allele in *K. pneumoniae* in France (2) and in the Netherlands (9). This difference might result from a lower capacity for bla_{KPC} encoding plasmids to conjugate to *E. coli* as compared to pOXA-48 or to a higher fitness cost. It might also be linked to sampling differences as different thresholds of carbapenem susceptibility might have been used to collect CRE isolates among studies. Indeed OXA-48-like carbapenemases are generally associated with lower levels of carbapenem resistance than KPC. This analysis was performed on isolates collected between 2012 and 2015 and revealed early trends in the evolution of CP-*Ec* isolated in France. It will be essential in the

331 characterization of the genomic evolution of CP-*Ec* in more recent years, which remains to be
332 performed.
333 The number of ARGs identified in the CP-*Ec* isolates from the F-NRC varied from one (the
334 carbapenemase gene only) to 26, showing that carbapenemase genes were acquired not only in MDR
335 isolates but also in an *E. coli* population that can be considered as "naïve" relative to an evolution
336 under antibiotic selective pressure and resident of the intestinal microbiota. This was particularly true
337 for isolates producing bla_{OXA-48} that were generally associated with a lower number of resistance genes
338 than isolates producing other carbapenemases, irrespectively of their clinical status (Fig. 4A). In
339 particular 118 out of the 121 (97.5%) isolates with no other ARG than the carbapenemase gene carried
340 bla_{OXA-48}. Therefore, the predominance of bla_{OXA-48} among the carbapenemase genes identified in the
341 F-NRC collection might mainly rely on the higher conjugative transfer rate of pOXA-48 related plasmids
342 compared to those encoding other carbapenemases (27). pOXA-48 has indeed been shown to rapidly
343 conjugate among *Enterobacterales* in hospitalized patients (28). This could also explain the high
344 frequency of bla_{OXA-48} carrying isolates belonging to ST10, ST69, ST88, ST127, ST12 and ST58 (Fig. 5),
345 that carried a small number of resistance genes and QRDR mutations and among which four were
346 previously identified among the most frequent *E. coli* ST characterized from fecal samples (29).
347 On the other hand, MDR CP-*Ec* isolates may result from the transfer of carbapenem resistance genes
348 into isolates already selected through multiple exposures to antibiotic treatments that have already
349 acquired multi-resistance plasmids or chromosomal mutations increasing their intrinsic drug
350 resistance, such as mutations in QRDR, in *ftsI* and/or in porin genes. Alternatively, the circulation of
351 carbapenem-resistant lineages, such as the OXA-181-producing ST410 *E. coli* lineage, showing a stable
352 association between the lineage and the resistance gene, may also occur and significantly contribute
353 to the number of CP-*Ec* isolates collected. Discriminating between both alternatives would require a
354 more extended comparison of plasmids carried in these lineages after long-read sequencing similarly
355 to what been done in *K. pneumoniae* (30). Strikingly, the analysis of *ftsI* alleles coding for a PBP3 with
356 the four amino-acid duplication revealed a contrasted situation among CP-*Ec* isolates collected in
357 France, with the duplication in *ftsI* found in 72.3%, 77.8% and 67% of the isolates carrying bla_{NDM-5}
358 (34/47), bla_{NDM-7} (7/9) and $bla_{OXA-181}$ (68/101) genes but in only 0.7% (4/458) of the isolates carrying
359 bla_{OXA-48}. We previously proposed that the fixation of mutations reducing the intrinsic susceptibiliy to
360 carbapenems might have favored the efficient conjugative transfer of plasmids carrying the
361 carbapenemase genes from other CPE species in the gut (10). Transconjugant would be selected in a
362 context of low biliary excretion of carbapenems or other ß-lactams after parenteral administration.
363 Increasing the proportion of the donor and recipient bacteria would therefore be less necessary for
364 plasmids with high conjugative rates, such as pOXA-48 (27). Alternatively, these mutations might also
365 have favored the plasmid maintenance by increasing the resistance level and selection of the isolates

366 during ß-lactam or carbapenem treament. Of particular concern in France are the OXA-181 producing
367 ST410 and the NDM (NDM-1, -5 and -7) ST167 lineages that significantly contribute to the circulation
368 of carbapenem resistance. However our study also reveals smaller lineages, that although less
369 frequently encountered in international studies, are nevertheless circulating. In contrast we did not
370 obtain evidence for clonal dissemination of CP-*Ec* ST131 lineages derived from the B2 clade responsible
371 for $bla_{\text{CTX-M-15}}$ gene dissemination (19, 20).
372 Despite their high frequency among the F-NRC collection, the ST38 isolates do not enter into one of
373 the two previous categories. Indeed, while they mainly express $bla_{\text{OXA-48}}$ or its single-point-mutant
374 derivative $bla_{\text{OXA-244}}$ (31), our phylogenetic analysis revealed that a majority of them belong to four
375 different lineages, including one mostly associated with a rapid dissemination in France. In contrast
376 with OXA-181 and NDM-producing lineages previously described, these lineages are associated with a
377 moderate number of ARGs and QRDR mutations. None of the ST38 isolates is mutated in *ftsI*, however
378 we previously demonstrated that all are characterized by an *ompC* allele that encodes a porin with a
379 reduced permeability to certain ß-lactams and has disseminated into unrelated lineages by
380 homologous recombination (10). A common feature of the four lineages is the integration of part of
381 the pOXA-48 plasmid carrying $bla_{\text{OXA-48}}$. This could have reduced a fitness cost of this plasmid and
382 facilitated the clonal expansion of these lineages. However, ST38 isolates were identified as
383 unfrequent colonizer of the GI tract (29, 32). Therefore additional features of these CP-*Ec* ST38 lineages
384 might have contributed to their dissemination.
385 In conclusion, by analysing genome sequences of CP-*Ec* isolates collected by the F-NRC we showed that
386 MDR lineages, enriched in carbapenemase-producing isolates are circulating in France, some of them,
387 such as ST1284 isolates being associated with outbreaks. It also suggests that the evolutionary
388 trajectory may depend on the carbapenemase gene, $bla_{\text{OXA-181}}$ or bla_{NDM} genes being more frequently
389 associated with the evolution of MDR *E. coli* lineages characterized by mutations in *ftsI* and *ompC*.
390 Surveillance of these mutations may be an important parameter in controling the circulation of MDR
391 lineages. On the other hand, carbapenemase genes are also frequently acquired through plasmid
392 dissemination from other bacterial species. Depending on the resistance background of the receiver
393 *E. coli*, this may lead to XDR or to isolates sensitive to a broad range of antibiotics. Finally, we also
394 observed a strong and rapid dissemination of ST38 isolates that might have been favored by a reduced
395 susceptibility to carbapenems linked to the ST38 *ompC* allele and by the chromosomal integration of
396 the carbapenemase gene. These results strengthen our model of different evolutionary trajectories
397 associated with the gain of carbapenemase genes (10). They also show that systematic genome
398 sequencing of CP-*Ec* and at a larger of CPE isolates, irrespective of their clinical or resistance status is
399 able to provide useful information not only on the circulation of MDR lineages, but also on the
400 propagation of resistance genes through horizontal gene transfer.

401

402 **MATERIAL AND METHODS**

403 **Isolate collection and sequencing.**

404 CP-*Ec* isolates analyzed in this study were collected by the F-NRC, mainly between the years 2012 to
405 2015. Twenty-two additional isolates we have received before the creation of the F-NRC in 2012, were
406 included in the analysis. Information on these isolates as the year of isolation, the region and
407 department in France and summary of their genomic features are reported in Table S1.

408

409 **Whole genome sequencing and analyses.**

410 DNA were extracted by using the Qiagen Blood and Tissue DNA easy kit. Sequencing libraries were
411 constructed by using the Nextera XT kit (Illumina) following the manufacturer instruction, and
412 sequenced with the Illumina HiSeq2500 or NextSeq500. FastQ files were trimmed for adaptors and
413 low-quality bases (setting the minimum base quality threshold to 25) with the Cutadapt fork Atropos
414 (33). *De novo* assemblies were generated from the trimmed reads with SPAdes v3.12.0 (34), using k-
415 mer sizes of 51, 71, 81, and 91, the coverage cut-off option was set to "auto" and the "careful" option
416 was activated. QUAST v2.2 (35) was used to assess the assembly quality and contigs shorter than 500
417 bp were filtered out for phylogenetic analyses. The ST38 isolates CNR65D6 and CNR85I8 were
418 sequenced to completion by using the long-read Pacbio technology. PacBio reads were assembled with
419 the RS_HGAP_Assembly.3 protocol from the SMRT analysis toolkit v2.3 (36) and with Canu (37),
420 polished with Quiver (36) and manually corrected by mapping Illumina reads using Breseq (38).
421 Assembled genomes were annotated with Prokka v1.9 (39). To analyze the F-NRC CP*Ec* isolates
422 belonging to the main ST recovered during the analysis in a more global context, their genome
423 sequences were combined to the assembled genome sequences from the same ST retrieved from the
424 NCBI database (July, 2019) and in some STs from Enterobase (http://enterobase.warwick.ac.uk/, April
425 2021). Retrieved genomes were annotated in the same way as the genome sequences of the F-NRC
426 isolates (Table S2).

427 To generate a core-genome phylogeny tree of all isolates, the best reference genome was first selected
428 among a set of 18 genomes analyzed by Touchon et al. (40) using the software refRank (41) and three
429 subsets of 100 randomly selected sequences from our study as an input. This led to the selection of
430 the genome sequence of strain MG1655-K12 (NC_000913.3) as the reference for read mapping and
431 SNP identification. Sequence reads for the 17 reference genomes (40) as well as for the genome
432 sequence of *Escherichia fergunsonii* strain ATCC 35469 (NC_011740.1), used as an outgroup were
433 simulated with ART (42). Trimmed sequencing reads were mapped against the MG1655-K12 genome
434 with BWA-MEM algorithm of the BWA v0.7.4 package (43). For SNP calling the Genome Analysis Toolkit
435 (GATK) v3.6.0 (44) was used with the following criteria, a minimum depth coverage (DP) of 10, a quality

436 by depth (QD) bigger than 2, a fisher strain bias (FS) below 60, a root mean square of the mapping
437 quality (MQ) above 40, and the mapping quality rank sum test (MQRankSum) and the read position
438 rank sum test (ReadPosRankSum) greater than -12.5 and -8 respectively. A Maximum-Likelihood tree
439 was estimated with RAxML v8.28 (45) using core-genome SNPs after removing positions in the
440 accessory genome identified with the filter_BSR_variome.py script from the LS-BSR pipeline (46).
441 For ST with more than 10 CP-*Ec* isolates from the F-NRC, a core genome alignment was generated with
442 Parsnp (47), by using a finished genome sequence as reference. A closely related isolate outside the
443 ST lineage was selected from the global phylogenetic tree including all F-NRC isolates and used as
444 outgroup to root the ST phylogenetic trees. Maximum-Likelihood (ML) trees were generated with
445 RAxML v8.28 (45) after removing regions of recombination with Gubbins (48). All graphic
446 representations were performed by using ITOL (49).
447
448 **MLST type, phylogroups, resistance gene and plasmid replicon identification.**
449 Sequence type was assigned to each assembly through a python script that relies on BLAST (10).
450 Antibiotic resistance genes (ARGs) and mutations in *gyrA, parC* and *parE* quinolone resistance
451 determining regions (QRDR) were identified with Resfinder 4.0 and PointFinder (50) run in local
452 respectively. The scripts and database (Retrieved: January 4, 2021) were downloaded from the
453 repositories of the Centre for Genomic Epidemiology (https://bitbucket.org/genomicepidemiology/).
454 The identified ARGs were manually reviewed to eliminate potential redundant ARG predicted at the
455 same genomic position. *mdf*(A) that is present in *E. coli* core genome was not taken into account.
456 Phylogroups were assigned by using EzClermont (51) run in local. Plasmid replicons were identified
457 with plasmidfinder run on each assembly (14). *ftsI*, *ompC and ompF* CDS sequences and *ompF*
458 promoter sequences were identified by using BlastN. Translated or nucleotide sequences were
459 clustered by cd-hit (cd-hit-v4.8.1) with an amino acid (FtsI, OmpC, OmpF) or nucleotide sequence
460 (*ompF* promoter) identity threshold of 1. Sequences of each cluster were aligned to detect mutations
461 in regions of interest: four amino-acid insertions between P333 and Y334 and E349K and I532L
462 mutations (FtsI), mutation modifying charge in L3 constriction loop, R195L mutation, nonsense or
463 frameshift mutations or OmpC sequence clustering with ST-38 OmpC sequences (OmpC), nonsense
464 mutations (OmpF) or mutations affecting one of the OmpR-boxes: mutation -46T/C in OmpR-F3 box
465 and mutation -75ΔT in OmpR-F2 box (*ompF* promoter).
466
467 **Determination of bla_{OXA-48} insertion site in ST38 clades 1, 2, 3 and 4**
468 The genome sequences of GCA_005886035.1 (CP040390.1), CNR65D6, GCA_004759025.1
469 (CP038505.1), and CNR85I8 were chosen as representative genomes of clusters 1, 3, 2 and 4,
470 respectively and aligned, by using Blastn, against the sequence of GCA_001900295.1 (CP010116.1), a

471 ST38 isolate that does not express a carbapenemase and whose genome sequence was complete. The
472 regions surrounding the *bla*$_{OXA-48}$ insertion sites in each clade were more precisely aligned against the
473 corresponding sequences of other representative genomes by using Easyfig (Easyfig_mac_2.1) (52)
474 (Fig. S3). To perform a blast analysis of insertion sites by using contigs generated from Illumina
475 sequences, smaller sequences were chosen as queries as following: nucleotides (nt)
476 1240133..1240934, nt 964173..965072, nt 419599..421606, nt 4206783..4207690 from
477 GCA_001900295.1 to screen for native sequences corresponding to the four *bla*$_{OXA-48}$ insertion site in
478 G1, G2, G3 and G4 clades and sequences nt 4460332..4460759 from CP040390.1, nt 4763987..4764506
479 from CNR65D6, nt 100784..102087 from CP038505.1 and nt 1206426..1206985 from CNR85I8 to
480 screen for the integration site plus IS*1* insertion as occurring in G1, G2, G3 and G4 clades respectively.
481
482 **Statistical analysis.**
483 Pearson's chi-squared tests were performed by using standard libraries contained within the R
484 statistics package (http://www.R-project.org)
485
486 **Availability of data.**
487 All sequence data have been deposited at DDBJ/EMBL/GenBank (BioProject PRJEB46636) and
488 bioSample identifiers for the Illumina sequence data are listed in Table S1. Complete genome
489 sequences of CNR65D6 and CNR85I8 and the long-read sequencing data have been deposited at
490 DDBJ/EMBL/GenBank with the accession number ERZ3517884 (PacBio reads, ERR6414227) and
491 ERZ3518335 (ERS6682837 PacBio reads) respectively.
492
493
494 **ACKNOWLEDGMENTS**
495 This work was supported by grants from the French National Research Agency (ANR-10-LABX-62-IBEID,
496 ANR-10-LABX-33, INCEPTION project (PIA/ANR-16-CONV-0005)) and from the European Union's
497 Horizon 2020 research and Innovation Program under grant agrement No 773830 (Project ARDIG, One
498 Health EJP). Pengdbamba Dieudonné Zongo is a scholar of Ed525 CDV, Sorbonne Université, Paris.
499
500 **REFERENCES**
501 1. Medina M, Castillo-Pino E. 2019. An introduction to the epidemiology and burden of urinary
502 tract infections. Ther Adv Urol 11:1756287219832172.
503 2. Dortet L, Cuzon G, Ponties V, Nordmann P. 2017. Trends in carbapenemase-producing
504 Enterobacteriaceae, France, 2012 to 2014. Euro Surveill 22.
505 3. French National Reference Centre for antibiotic resistance, activity report 2019 - 2020.
506 https://wwwcnr-resistance-antibiotiquesfr/bilans-dactivitehtml.

507 4. Saleem AF, Allana A, Hale L, Diaz A, Salinas R, Salinas C, Qureshi SM, Hotwani A, Rahman N,
508 Khan A, Zaidi AK, Seed PC, Arshad M. 2020. The Gut of Healthy Infants in the Community as a
509 Reservoir of ESBL and Carbapenemase-Producing Bacteria. Antibiotics (Basel) 9:286.
510 5. Bush K, Jacoby GA. 2010. Updated functional classification of beta-lactamases. Antimicrob
511 Agents Chemother 54:969-76.
512 6. Stoesser N, Sheppard AE, Pankhurst L, De Maio N, Moore CE, Sebra R, Turner P, Anson LW,
513 Kasarskis A, Batty EM, Kos V, Wilson DJ, Phetsouvanh R, Wyllie D, Sokurenko E, Manges AR,
514 Johnson TJ, Price LB, Peto TE, Johnson JR, Didelot X, Walker AS, Crook DW. 2016. Evolutionary
515 History of the Global Emergence of the *Escherichia coli* Epidemic Clone ST131. MBio 7:e02162.
516 7. Gauthier L, Dortet L, Cotellon G, Creton E, Cuzon G, Ponties V, Bonnin RA, Naas T. 2018.
517 Diversity of carbapenemase-producing *Escherichia coli* isolates, France 2012-2013. Antimicrob
518 Agents Chemother doi:10.1128/aac.00266-18.
519 8. Ellaby N, Doumith M, Hopkins KL, Woodford N, Ellington MJ. 2019. Emergence of diversity in
520 carbapenemase-producing *Escherichia coli* ST131, England, January 2014 to June 2016. Euro
521 Surveill 24:1800627
522 9. van der Zwaluw K, Witteveen S, Wielders L, van Santen M, Landman F, de Haan A, Schouls LM,
523 Bosch T. 2020. Molecular characteristics of carbapenemase-producing *Enterobacterales* in the
524 Netherlands; results of the 2014-2018 national laboratory surveillance. Clin Microbiol Infect
525 26:1412.e7-1412.e12.
526 10. Patino-Navarrete R, Rosinski-Chupin I, Cabanel N, Gauthier L, Takissian J, Madec JY, Hamze M,
527 Bonnin RA, Naas T, Glaser P. 2020. Stepwise evolution and convergent recombination underlie
528 the global dissemination of carbapenemase-producing *Escherichia coli*. Genome Med 12:10.
529 11. Roer L, Overballe-Petersen S, Hansen F, Schønning K, Wang M, Røder BL, Hansen DS, Justesen
530 US, Andersen LP, Fulgsang-Damgaard D, Hopkins KL, Woodford N, Falgenhauer L, Chakraborty
531 T, Samuelsen Ø, Sjöström K, Johannesen TB, Ng K, Nielsen J, Ethelberg S, Stegger M,
532 Hammerum AM, Hasman H. 2018. *Escherichia coli* Sequence Type 410 Is Causing New
533 International High-Risk Clones. mSphere 3:e00337-18
534 12. Beghain J, Bridier-Nahmias A, Le Nagard H, Denamur E, Clermont O. 2018. ClermonTyping: an
535 easy-to-use and accurate *in silico* method for *Escherichia* genus strain phylotyping. Microb
536 Genom 4:0.000192
537 13. Hendrickx APA, Landman F, de Haan A, Witteveen S, van Santen-Verheuvel MG, Schouls LM,
538 The Dutch Cpe Surveillance Study G. 2021. bla (OXA-48)-like genome architecture among
539 carbapenemase-producing *Escherichia coli* and *Klebsiella pneumoniae* in the Netherlands.
540 Microb Genom 7:000512
541 14. Carattoli A, Zankari E, Garcia-Fernandez A, Voldby Larsen M, Lund O, Villa L, Moller Aarestrup
542 F, Hasman H. 2014. In silico detection and typing of plasmids using PlasmidFinder and plasmid
543 multilocus sequence typing. Antimicrob Agents Chemother 58:3895-903.
544 15. Turton JF, Doumith M, Hopkins KL, Perry C, Meunier D, Woodford N. 2016. Clonal expansion
545 of *Escherichia coli* ST38 carrying a chromosomally integrated OXA-48 carbapenemase gene. J
546 Med Microbiol 65:538-46.
547 16. Leverstein-van Hall MA, Dierikx CM, Cohen Stuart J, Voets GM, van den Munckhof MP, van
548 Essen-Zandbergen A, Platteel T, Fluit AC, van de Sande-Bruinsma N, Scharinga J, Bonten MJ,
549 Mevius DJ. 2011. Dutch patients, retail chicken meat and poultry share the same ESBL genes,
550 plasmids and strains. Clin Microbiol Infect 17:873-80.
551 17. Oteo J, Diestra K, Juan C, Bautista V, Novais A, Pérez-Vázquez M, Moyá B, Miró E, Coque TM,
552 Oliver A, Cantón R, Navarro F, Campos J. 2009. Extended-spectrum beta-lactamase-producing
553 *Escherichia coli* in Spain belong to a large variety of multilocus sequence typing types, including
554 ST10 complex/A, ST23 complex/A and ST131/B2. Int J Antimicrob Agents 34:173-6.
555 18. Manges AR, Mende K, Murray CK, Johnston BD, Sokurenko EV, Tchesnokova V, Johnson JR.
556 2017. Clonal distribution and associated characteristics of *Escherichia coli* clinical and
557 surveillance isolates from a military medical center. Diagn Microbiol Infect Dis 87:382-385.

558 19. Price LB, Johnson JR, Aziz M, Clabots C, Johnston B, Tchesnokova V, Nordstrom L, Billig M,
559 Chattopadhyay S, Stegger M, Andersen PS, Pearson T, Riddell K, Rogers P, Scholes D, Kahl B,
560 Keim P, Sokurenko EV. 2013. The Epidemic of Extended-Spectrum-beta-Lactamase-Producing
561 *Escherichia coli* ST131 Is Driven by a Single Highly Pathogenic Subclone, H30-Rx. MBio
562 4:e00377-13
563 20. Nicolas-Chanoine MH, Bertrand X, Madec JY. 2014. *Escherichia coli* ST131, an intriguing clonal
564 group. Clin Microbiol Rev 27:543-74.
565 21. Decano AG, Downing T. 2019. An *Escherichia coli* ST131 pangenome atlas reveals population
566 structure and evolution across 4,071 isolates. Sci Rep 9:17394.
567 22. Potron A, Bernabeu S, Cuzon G, Pontiès V, Blanchard H, Seringe E, Naas T, Nordmann P, Dortet
568 L. 2017. Analysis of OXA-204 carbapenemase-producing Enterobacteriaceae reveals possible
569 endoscopy-associated transmission, France, 2012 to 2014. Euro Surveill 22:17-00048
570 23. Lepelletier D, Berthelot P, Lucet JC, Fournier S, Jarlier V, Grandbastien B. 2015. French
571 recommendations for the prevention of 'emerging extensively drug-resistant bacteria' (eXDR)
572 cross-transmission. J Hosp Infect 90:186-95.
573 24. Ortega A, Sáez D, Bautista V, Fernández-Romero S, Lara N, Aracil B, Pérez-Vázquez M, Campos
574 J, Oteo J. 2016. Carbapenemase-producing *Escherichia coli* is becoming more prevalent in
575 Spain mainly because of the polyclonal dissemination of OXA-48. J Antimicrob Chemother
576 71:2131-8.
577 25. Grundmann H, Glasner C, Albiger B, Aanensen DM, Tomlinson CT, Andrasević AT, Cantón R,
578 Carmeli Y, Friedrich AW, Giske CG, Glupczynski Y, Gniadkowski M, Livermore DM, Nordmann
579 P, Poirel L, Rossolini GM, Seifert H, Vatopoulos A, Walsh T, Woodford N, Monnet DL. 2017.
580 Occurrence of carbapenemase-producing *Klebsiella pneumoniae* and *Escherichia coli* in the
581 European survey of carbapenemase-producing Enterobacteriaceae (EuSCAPE): a prospective,
582 multinational study. Lancet Infect Dis 17:153-163.
583 26. David S, Reuter S, Harris SR, Glasner C, Feltwell T, Argimon S, Abudahab K, Goater R, Giani T,
584 Errico G, Aspbury M, Sjunnebo S, Feil EJ, Rossolini GM, Aanensen DM, Grundmann H. 2019.
585 Epidemic of carbapenem-resistant *Klebsiella pneumoniae* in Europe is driven by nosocomial
586 spread. Nat Microbiol 4:1919-1929.
587 27. Potron A, Poirel L, Nordmann P. 2014. Derepressed transfer properties leading to the efficient
588 spread of the plasmid encoding carbapenemase OXA-48. Antimicrob Agents Chemother
589 58:467-71.
590 28. León-Sampedro R, DelaFuente J, Díaz-Agero C, Crellen T, Musicha P, Rodríguez-Beltrán J, de la
591 Vega C, Hernández-García M, López-Fresneña N, Ruiz-Garbajosa P, Cantón R, Cooper BS, San
592 Millán Á. 2021. Pervasive transmission of a carbapenem resistance plasmid in the gut
593 microbiota of hospitalized patients. Nat Microbiol 6:606-616.
594 29. Matsui Y, Hu Y, Rubin J, de Assis RS, Suh J, Riley LW. 2020. Multilocus sequence typing of
595 *Escherichia coli* isolates from urinary tract infection patients and from fecal samples of healthy
596 subjects in a college community. Microbiologyopen 9:1225-1233.
597 30. David S, Cohen V, Reuter S, Sheppard AE, Giani T, Parkhill J, Rossolini GM, Feil EJ, Grundmann
598 H, Aanensen DM. 2020. Integrated chromosomal and plasmid sequence analyses reveal
599 diverse modes of carbapenemase gene spread among *Klebsiella pneumoniae*. Proc Natl Acad
600 Sci U S A 117:25043-25054.
601 31. Emeraud C, Girlich D, Bonnin RA, Jousset AB, Naas T, Dortet L. 2021. Emergence and Polyclonal
602 Dissemination of OXA-244-Producing *Escherichia coli*, France. Emerg Infect Dis 27:1206-1210.
603 32. Massot M, Daubié AS, Clermont O, Jauréguy F, Couffignal C, Dahbi G, Mora A, Blanco J, Branger
604 C, Mentré F, Eddi A, Picard B, Denamur E, The Coliville G. 2016. Phylogenetic, virulence and
605 antibiotic resistance characteristics of commensal strain populations of *Escherichia coli* from
606 community subjects in the Paris area in 2010 and evolution over 30 years. Microbiology
607 (Reading) 162:642-650.
608 33. Didion JP, Martin M, Collins FS. 2017. Atropos: specific, sensitive, and speedy trimming of
609 sequencing reads. PeerJ 5:e3720.

610 34. Bankevich A, Nurk S, Antipov D, Gurevich AA, Dvorkin M, Kulikov AS, Lesin VM, Nikolenko SI,
611 Pham S, Prjibelski AD, Pyshkin AV, Sirotkin AV, Vyahhi N, Tesler G, Alekseyev MA, Pevzner PA.
612 2012. SPAdes: a new genome assembly algorithm and its applications to single-cell
613 sequencing. J Comput Biol 19:455-77.
614 35. Gurevich A, Saveliev V, Vyahhi N, Tesler G. 2013. QUAST: quality assessment tool for genome
615 assemblies. Bioinformatics 29:1072-5.
616 36. Chin CS, Alexander DH, Marks P, Klammer AA, Drake J, Heiner C, Clum A, Copeland A,
617 Huddleston J, Eichler EE, Turner SW, Korlach J. 2013. Nonhybrid, finished microbial genome
618 assemblies from long-read SMRT sequencing data. Nat Methods 10:563-9.
619 37. Koren S, Walenz BP, Berlin K, Miller JR, Bergman NH, Phillippy AM. 2017. Canu: scalable and
620 accurate long-read assembly via adaptive k-mer weighting and repeat separation. Genome Res
621 27:722-736.
622 38. Deatherage DE, Barrick JE. 2014. Identification of mutations in laboratory-evolved microbes
623 from next-generation sequencing data using breseq. Methods Mol Biol 1151:165-88.
624 39. Seemann T. 2014. Prokka: rapid prokaryotic genome annotation. Bioinformatics 30:2068-9.
625 40. Touchon M, Hoede C, Tenaillon O, Barbe V, Baeriswyl S, Bidet P, Bingen E, Bonacorsi S,
626 Bouchier C, Bouvet O, Calteau A, Chiapello H, Clermont O, Cruveiller S, Danchin A, Diard M,
627 Dossat C, Karoui ME, Frapy E, Garry L, Ghigo JM, Gilles AM, Johnson J, Le Bouguenec C, Lescat
628 M, Mangenot S, Martinez-Jehanne V, Matic I, Nassif X, Oztas S, Petit MA, Pichon C, Rouy Z, Ruf
629 CS, Schneider D, Tourret J, Vacherie B, Vallenet D, Medigue C, Rocha EP, Denamur E. 2009.
630 Organised genome dynamics in the *Escherichia coli* species results in highly diverse adaptive
631 paths. PLoS Genet 5:e1000344.
632 41. Becker L, Fuchs S, Pfeifer Y, Semmler T, Eckmanns T, Korr G, Sissolak D, Friedrichs M, Zill E,
633 Tung ML, Dohle C, Kaase M, Gatermann S, Rüssmann H, Steglich M, Haller S, Werner G. 2018.
634 Whole Genome Sequence Analysis of CTX-M-15 Producing *Klebsiella Isolates* Allowed
635 Dissecting a Polyclonal Outbreak Scenario. Front Microbiol 9:322.
636 42. Huang W, Li L, Myers JR, Marth GT. 2012. ART: a next-generation sequencing read simulator.
637 Bioinformatics 28:593-4.
638 43. Li H, Durbin R. 2009. Fast and accurate short read alignment with Burrows-Wheeler transform.
639 Bioinformatics 25:1754-60.
640 44. McKenna A, Hanna M, Banks E, Sivachenko A, Cibulskis K, Kernytsky A, Garimella K, Altshuler
641 D, Gabriel S, Daly M, DePristo MA. 2010. The Genome Analysis Toolkit: a MapReduce
642 framework for analyzing next-generation DNA sequencing data. Genome Res 20:1297-303.
643 45. Stamatakis A. 2014. RAxML version 8: a tool for phylogenetic analysis and post-analysis of large
644 phylogenies. Bioinformatics 30:1312-3.
645 46. Sahl JW, Caporaso JG, Rasko DA, Keim P. 2014. The large-scale blast score ratio (LS-BSR)
646 pipeline: a method to rapidly compare genetic content between bacterial genomes. PeerJ
647 2:e332.
648 47. Treangen TJ, Ondov BD, Koren S, Phillippy AM. 2014. The Harvest suite for rapid core-genome
649 alignment and visualization of thousands of intraspecific microbial genomes. Genome Biol
650 15:524.
651 48. Croucher NJ, Page AJ, Connor TR, Delaney AJ, Keane JA, Bentley SD, Parkhill J, Harris SR. 2015.
652 Rapid phylogenetic analysis of large samples of recombinant bacterial whole genome
653 sequences using Gubbins. Nucleic Acids Res 43:e15.
654 49. Letunic I, Bork P. 2019. Interactive Tree Of Life (iTOL) v4: recent updates and new
655 developments. Nucleic Acids Res 47:W256-w259.
656 50. Bortolaia V, Kaas RS, Ruppe E, Roberts MC, Schwarz S, Cattoir V, Philippon A, Allesoe RL, Rebelo
657 AR, Florensa AF, Fagelhauer L, Chakraborty T, Neumann B, Werner G, Bender JK, Stingl K,
658 Nguyen M, Coppens J, Xavier BB, Malhotra-Kumar S, Westh H, Pinholt M, Anjum MF, Duggett
659 NA, Kempf I, Nykäsenoja S, Olkkola S, Wieczorek K, Amaro A, Clemente L, Mossong J, Losch S,
660 Ragimbeau C, Lund O, Aarestrup FM. 2020. ResFinder 4.0 for predictions of phenotypes from
661 genotypes. J Antimicrob Chemother doi:10.1093/jac/dkaa345.

662 51. Waters NR, Abram F, Brennan F, Holmes A, Pritchard L. 2020. Easy phylotyping of Escherichia
663 coli via the EzClermont web app and command-line tool. Access Microbiol 2:acmi000143.
664 52. Sullivan MJ, Petty NK, Beatson SA. 2011. Easyfig: a genome comparison visualizer.
665 Bioinformatics 27:1009-10.
666
667

668 **Figure legends**

669 **Figure 1. Origin of the isolates received by the F-NRC during the 2012-2015 period**. **A**. Absolute
670 number of isolates per year from infection, screening or unknown origins, differentiating between
671 isolates that have or not been sequenced. **B**. Proportions of isolates from infection or from screening
672 or unknown origins showing that isolates from infection origin represent the same proportions among
673 total isolates that have been received by the F-NRC and isolates that have sequenced.
674

675 **Figure 2: Core genome phylogeny of CP-*Ec* isolates received by the F-NRC**. ML phylogeny of the 713
676 CP-*Ec* isolates was built with RAxML (45) from 372,238 core SNPs after sequence alignment on
677 MG1655-K12 (NC_000913.3) selected as the best reference. The genome sequence of *Escherichia*
678 *fergunsonii* strain ATCC 35469 (NC_011740.1) was used as an outgroup for the phylogenetic analysis.
679 Genomes from Touchon et al. (40) were also incorporated into the analysis. Genomic features are
680 indicated as in the figure key (left) from the inside to the outside circles: carbapenemases of the OXA,
681 NDM and other types, CTX-M ESBL, mutations in *gyrA* and *parC* QRDR region (FQ resistance), origin,
682 main ST, phylogroups. Reference genome from Touchon *et al*. are indicated as Touchon.
683

684 **Figure 3. Resistance gene content of the F-NRC CP-*Ec* isolates**. **A**. Box plot representation of the ARGs
685 content according to the phylogroup. The number of isolates belonging to each phylogroup is indicated
686 between brackets. The limits of the box indicate the lower and upper quartile. Outliers are indicated
687 by points above the maximal value. **B**: Relationships between the ARGs number and the number of
688 mutations in QRDR. In the box plot representations, the median is indicated by an horizontal bar and
689 the mean by a cross.
690

691 **Figure 4. Carbapenemase gene content of the F-NRC CP-*Ec* isolates**. **A**. Relationship between the
692 carbapenemase allele and the ARGs content. In the box plot representation, the median is indicated
693 by an horizontal bar and the mean by a cross. The limits of the box indicate the lower and upper
694 quartile. Outliers are indicated by points above the maximal value. **B**. Number of isolates carrying a
695 specific carbapenemase allele according to the number of QRDR mutations in their genomes. **C**. Per-
696 year evolution of the percentage of isolates carrying the different carbapenemase alleles in the 2012-

697 2015 period. Year of isolation are indicated as in the figure key (right). Given their small number (n=22),
698 strains isolated before 2012 are not indicated**.**
699
700 **Figure 5**. Features of the main ST associated with CP-*Ec* isolates in France. **A**. Proportion of the isolates
701 according to the carbapenemase allele in each ST; **B**. Box plot representation of the ARGs content
702 according to the ST; **C.** Proportion of isolates according to the number of mutations in QRDR; **D** :
703 Proportion of isolates with a specific PBP3 allele. PBP3 characterized by a YRIP, YRIK or YRIN insertion
704 between positions 333 and 334, the YRIN insertion is generally associated with a A413V mutation
705 (YRIN-L) and less frequently with a E349K mutation (YRIN-K-L) (10); **E.** Proportion of isolates carrying
706 specific mutations in *ompC:* R195L, G138D or acquisition of a ST38-like *ompC* allele by recombination
707 (10). For each ST, the phylogroup, the total number of isolates and the number of isolates associated
708 with urinary tract infections are indicated in the upper panel. Intermediate (Inter) and minor ST
709 indicate ST represented by 4-6 and 1-3 isolates, respectively.
710
711 **Figure 6. Core genome phylogeny of ST38 isolates.** ML Phylogeny was based on genome sequences
712 of 92 CP-*Ec* from the F-NRC and 464 genome sequences retrieved from Enterobase and from the NCBI
713 database including 331 carrying a carbapenemase gene. A core genome (2,900,000 nt) alignment of
714 the *de novo* assemblies on the sequence of GCA_005886035.1 used as a reference was performed by
715 using Parsnp (47); ML phylogeny was built with RAxML (45) from 6,170 core SNPs after removing
716 recombined regions with Gubbins (48). The genome sequence of CNRC6O47 (ST963) was used as an
717 outgroup for the phylogenetic analysis. F-NRC isolates are indicated by red triangles (inner circle).
718 Other genomic features are indicated as indicated in the figure key (left) from the inside to the outside
719 circles: carbapenemases of the OXA, NDM and other types, absence of any plasmid of any Inc-type as
720 identified by using PlasmidFinder (14), ESBL of the CTX-M types, number of mutations in *gyrA* and *parC*
721 QRDRs (FQ resistance), number of ARGs, mutations in *ftsI*, *ompC*, *ompF*, geographical origin. The four
722 OXA-48-like clades (G1, G2, G3, G4) clustering most French isolates are colored in blue, red, violet and
723 green. A fifth clade (G5) corresponding to a possible outbreak of VIM-4 isolates in the East of Paris is
724 colored in brown
725
726 **Figure 7**. ***bla*$_{\text{OXA-48}}$ integration sites of ST38 CP-*Ec* clades 1, 2, 3 and 4.** The genome sequences of
727 GCA_005886035.1 (CP040390.1), CNR65D6, GCA_004759025.1 (CP038505.1), and CNR85I8 were
728 chosen as representative genomes of clusters 1, 2, 3 and 4, respectively and aligned, by using Blastn,
729 against the sequence of GCA_001900295.1 (CP010116.1), a ST38 isolate that does not carry a
730 carbapenemase gene and whose genome sequence was complete. Gene annotations were derived
731 from MG1655 (NC_000913.3). The regions surrounding the *bla*$_{\text{OXA-48}}$ insertion sites in each clade were

732 more precisely aligned against the corresponding sequences of CP010116.1 and of representative
733 genomes of the other clades by using Easyfig (52). *bla*$_{OXA-48}$ is represented by a brown arrow,
734 cointegrated genes of pOXA-48 origin with light green arrows and the IS*1* transposase with a green
735 arrow. Sequences used to perform the BLAST analysis on Illumina contigs are underlined in red. It is to
736 note that, in the G3 clade, *bla*$_{OXA-48}$ integration occurs into a genomic island inserted at tRNASer.
737 Another genomic island is present in G1-type strains but does not carry *bla*$_{OXA-48}$.
738
739

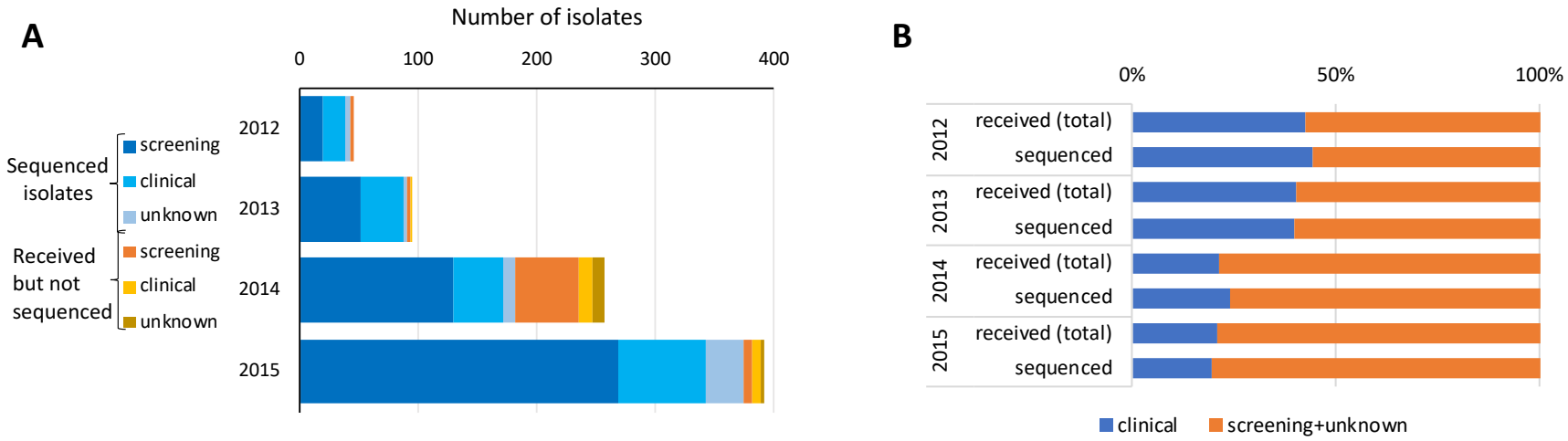
A
Number of isolates
0
100
200
300
400
2012
2013
2014
2015
Sequenced isolates
screening
clinical
unknown
Received but not sequenced
screening
clinical
unknown
B
0%
50%
100%
received (total)
sequenced
2012
2013
2014
2015
clinical
screening+unknown

Fig.1

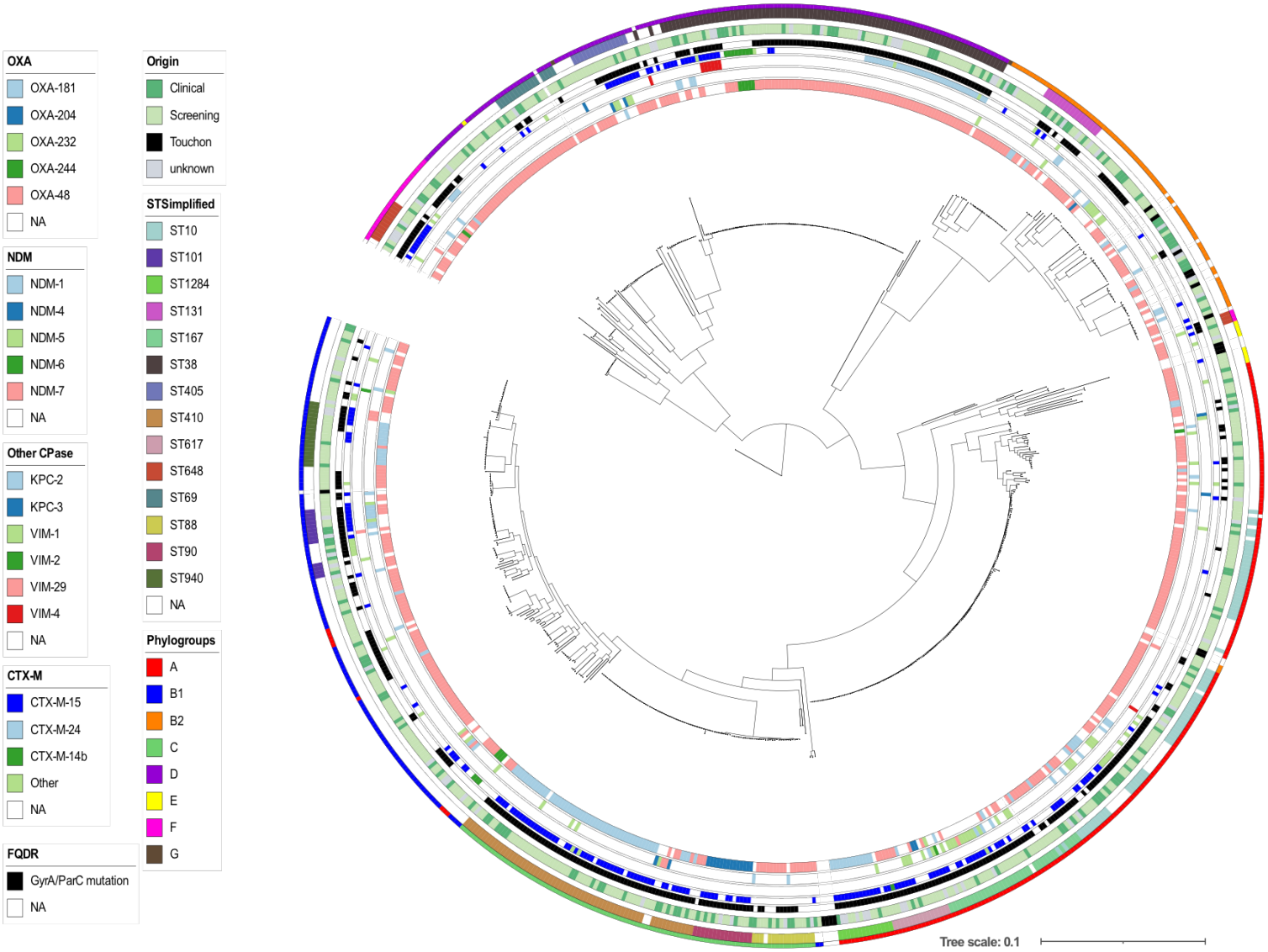
OXA
OXA-181
OXA-204
OXA-232
OXA-244
OXA-48
NA
NDM
NDM-1
NDM-4
NDM-5
NDM-6
NDM-7
NA
Other CPase
KPC-2
KPC-3
VIM-1
VIM-2
VIM-29
VIM-4
NA
CTX-M
CTX-M-15
CTX-M-24
CTX-M-14b
Other
NA
FQDR
GyrA/ParC mutation
NA
Origin
Clinical
Screening
Touchon
unknown
STSimplified
ST10
ST101
ST1284
ST131
ST167
ST38
ST405
ST410
ST617
ST648
ST69
ST88
ST90
ST940
NA
Phylogroups
A
B1
B2
C
D
E
F
G
Tree scale: 0.1

Fig.2

A

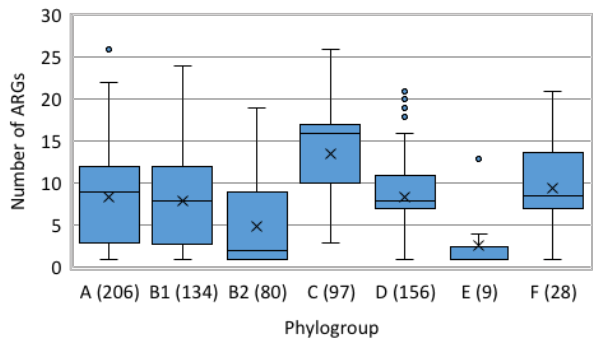
30
25
20
15
10
5
0
Number of ARGs
A (206)
B1 (134)
B2 (80)
C (97)
D (156)
E (9)
F (28)
Phylogroup

B

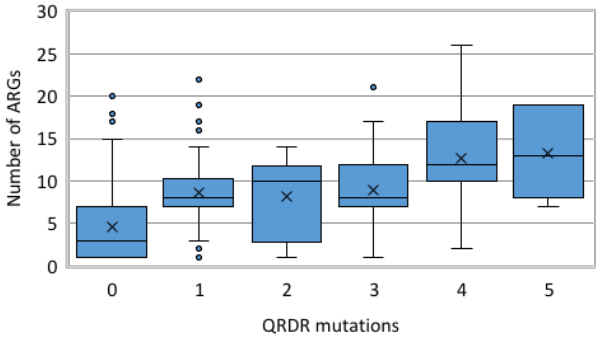
30
25
20
15
10
5
0
Number of ARGs
0
1
2
3
4
5
QRDR mutations

Fig.3

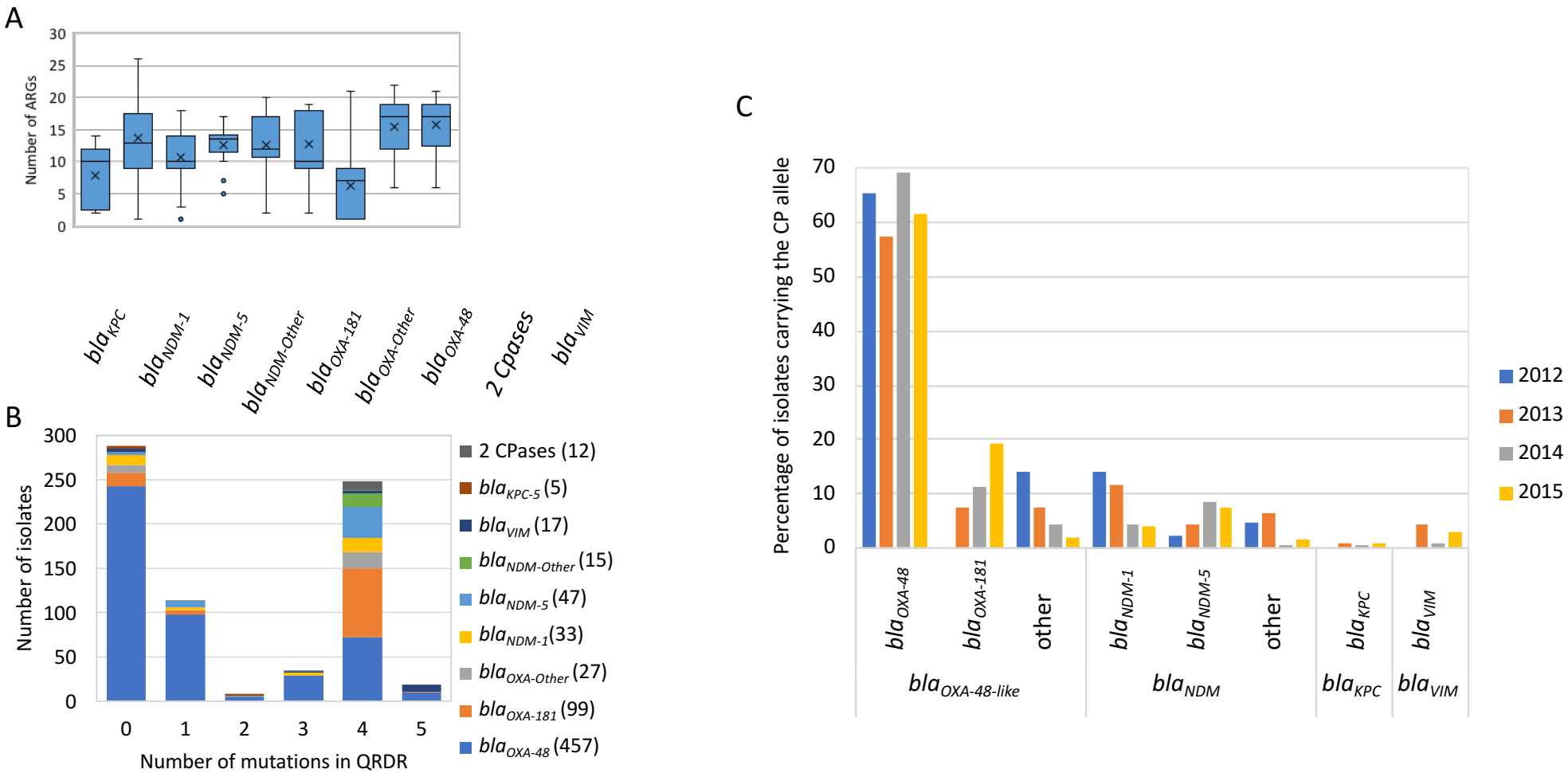
A
Number of ARGs
30
25
20
15
10
5
0
bla KPC
bla NDM-1
bla NDM-5
bla NDM-Other
bla OXA-181
bla OXA-Other
bla OXA-48
2 Cpases
bla VIM
B
Number of isolates
300
250
200
150
100
50
0
0
1
2
3
4
5
Number of mutations in QRDR
2 CPases (12)
bla KPC-5 (5)
bla VIM (17)
bla NDM-Other (15)
bla NDM-5 (47)
bla NDM-1 (33)
bla OXA-Other (27)
bla OXA-181 (99)
bla OXA-48 (457)
C
Percentage of isolates carrying the CP allele
70
60
50
40
30
20
10
0
bla OXA-48
bla OXA-181
other
bla NDM-1
bla NDM-5
other
bla KPC
bla VIM
bla OXA-48-like
bla NDM
bla KPC
bla VIM
2012
2013
2014
2015

Fig.4

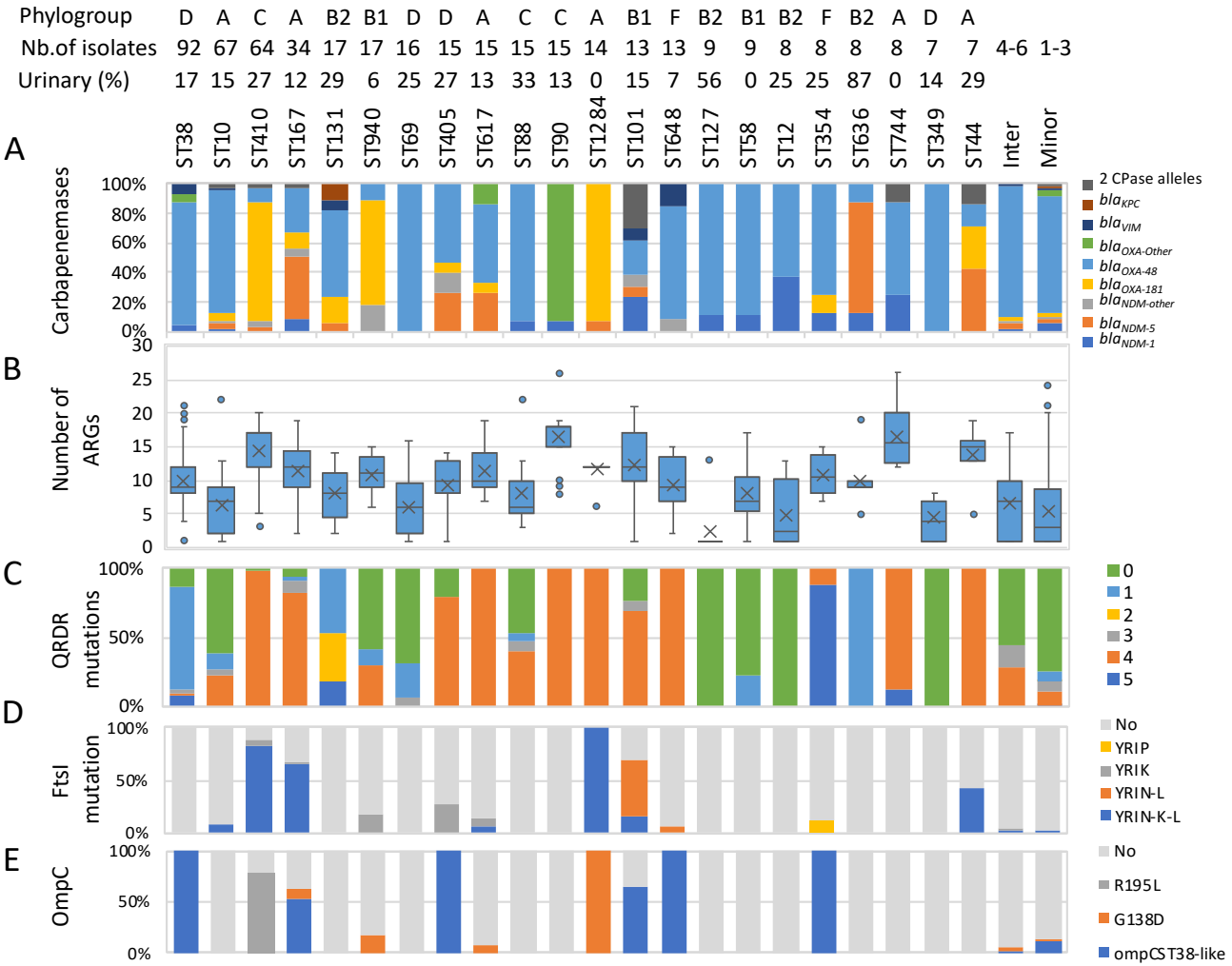
Phylogroup D A C A B2 B1 D D A C C A B1 F B2 B1 B2 F B2 A D A
Nb.of isolates 92 67 64 34 17 17 16 15 15 15 15 14 13 13 9 9 8 8 8 8 7 7 4-6 1-3
Urinary (%) 17 15 27 12 29 6 25 27 13 33 13 0 15 7 56 0 25 25 87 0 14 29
ST38 ST10 ST410 ST167 ST131 ST940 ST69 ST405 ST617 ST88 ST90 ST1284 ST101 ST648 ST127 ST58 ST12 ST354 ST636 ST744 ST349 ST44 Inter Minor
A
Carbapenemases
100%
80%
60%
40%
20%
0%
2 CPase alleles
bla KPC
bla VIM
bla OXA-Other
bla OXA-48
bla OXA-181
bla NDM-other
bla NDM-5
bla NDM-1
B
Number of ARGs
30
25
20
15
10
5
0
C
QRDR mutations
100%
50%
0%
0
1
2
3
4
5
D
FtsI mutation
100%
50%
0%
No
YRIP
YRIK
YRIN-L
YRIN-K-L
E
OmpC
100%
50%
0%
No
R195L
G138D
ompCST38-like

Fig. 5

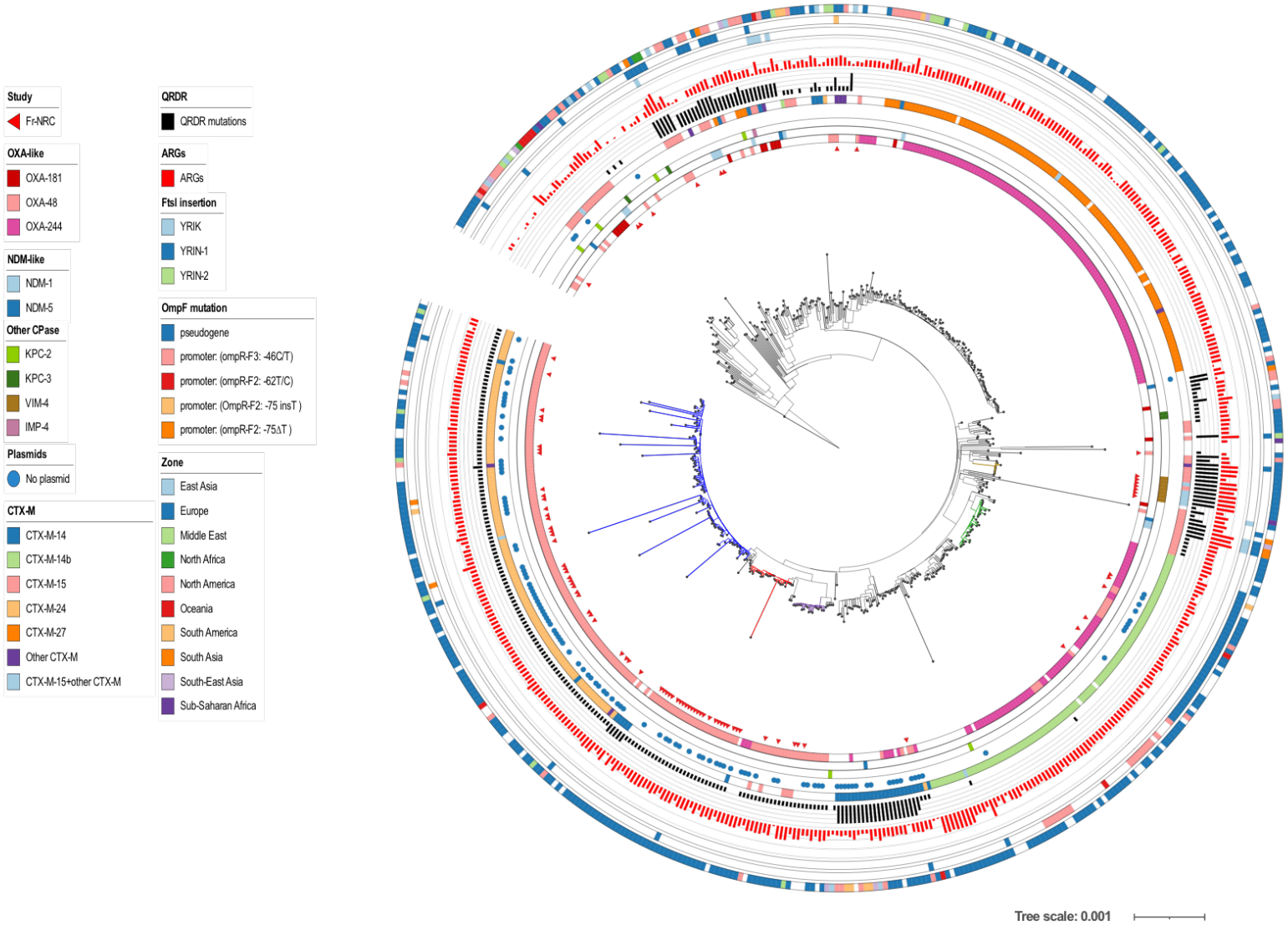
Study
Fr-NRC
OXA-like
OXA-181
OXA-48
OXA-244
NDM-like
NDM-1
NDM-5
Other CPase
KPC-2
KPC-3
VIM-4
IMP-4
Plasmids
No plasmid
CTX-M
CTX-M-14
CTX-M-14b
CTX-M-15
CTX-M-24
CTX-M-27
Other CTX-M
CTX-M-15+other CTX-M
QRDR
QRDR mutations
ARGs
ARGs
FtsI insertion
YRIK
YRIN-1
YRIN-2
OmpF mutation
pseudogene
promoter: (ompR-F3: -46C/T)
promoter: (ompR-F2: -62T/C)
promoter: (OmpR-F2: -75 insT)
promoter: (ompR-F2: -75ΔT)
Zone
East Asia
Europe
Middle East
North Africa
North America
Oceania
South America
South Asia
South-East Asia
Sub-Saharan Africa
Tree scale: 0.001

Fig.6

G1-type insertion

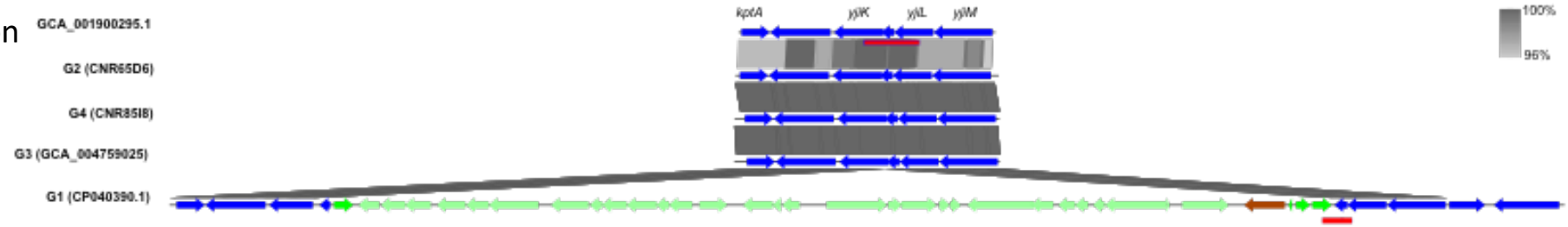

G2-type insertion

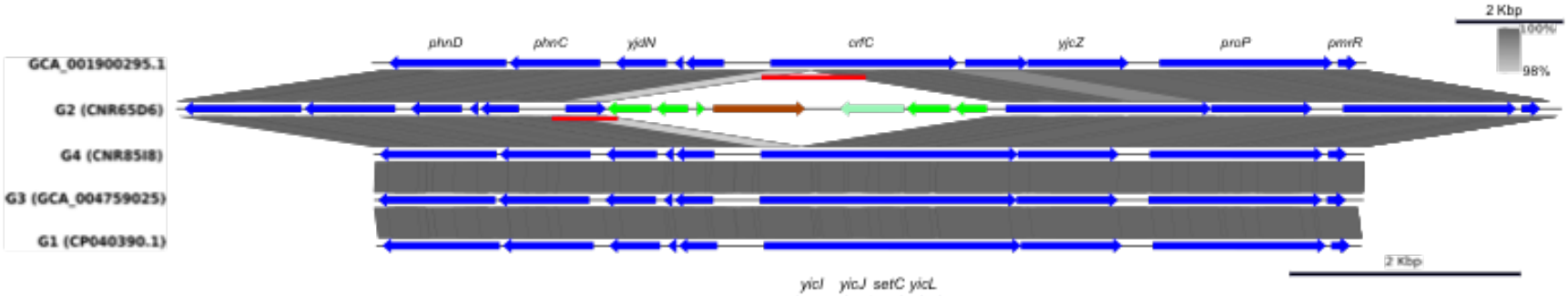

G3-type insertion

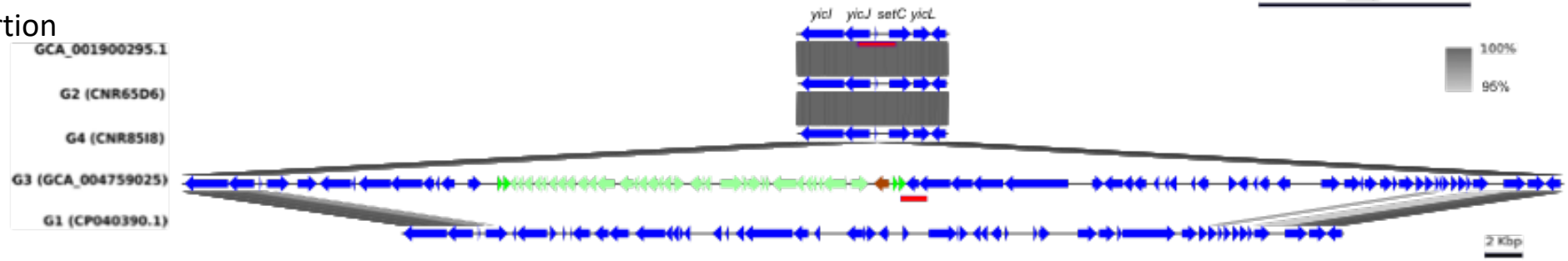

G4-type insertion

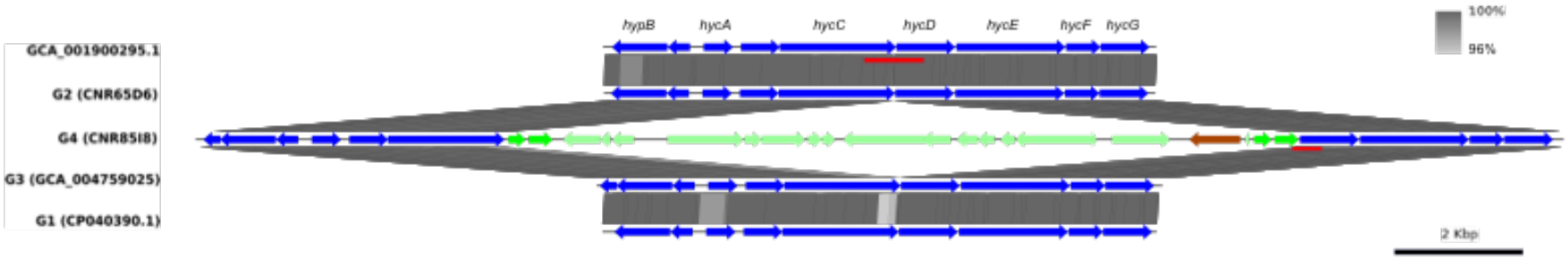

Fig. 7

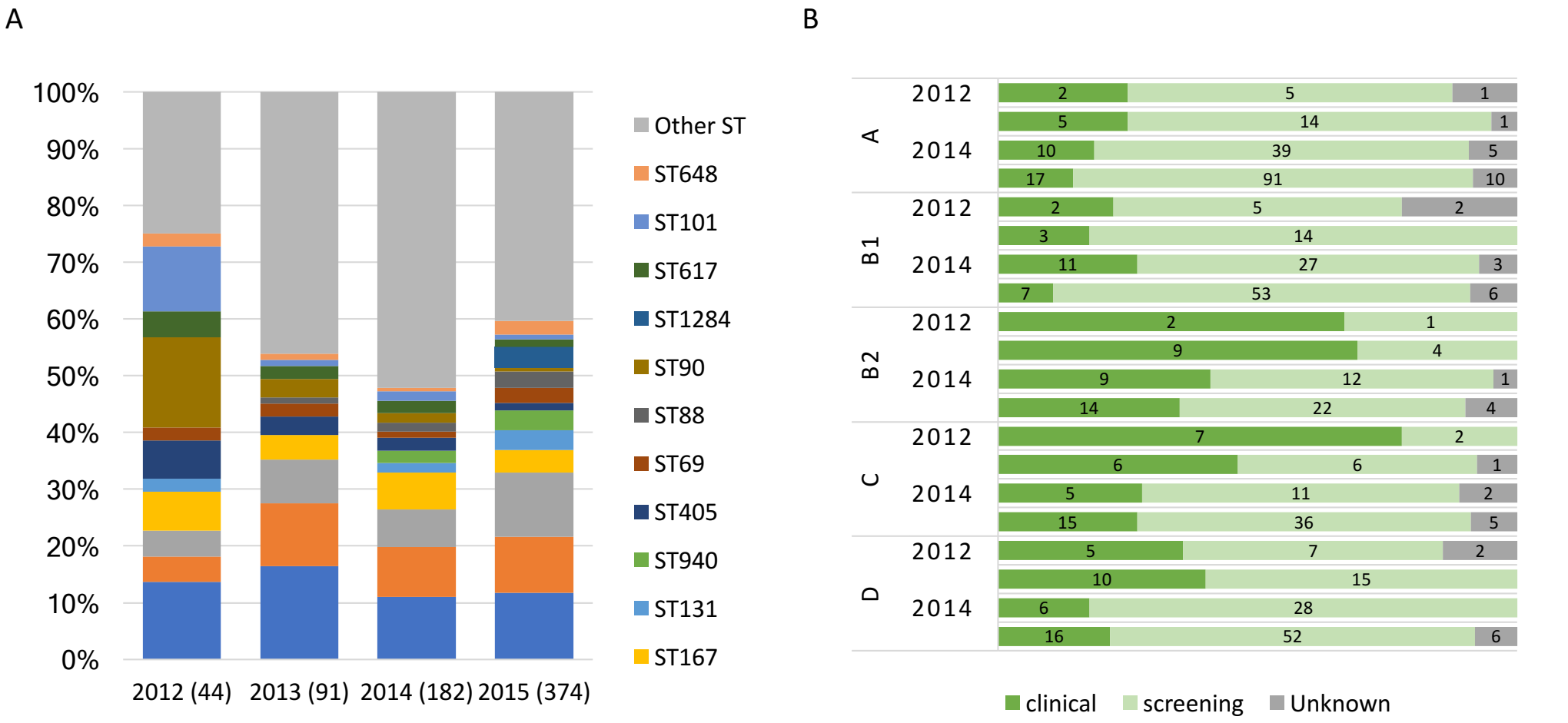

Figure S1. **Per-year analysis of the origin of the isolates received by the F-NRC. A**. Proportions of the isolates belonging to the different ST. The total number of isolates is indicated between brackets. The large proportion of ST90 isolates collected in 2012 is linked to a local outbreak. **B**. Proportions of the isolates collected in screening and infection situations as a function of the year and the phylogroup. The absolute number of isolates for each class is indicated inside the bars.

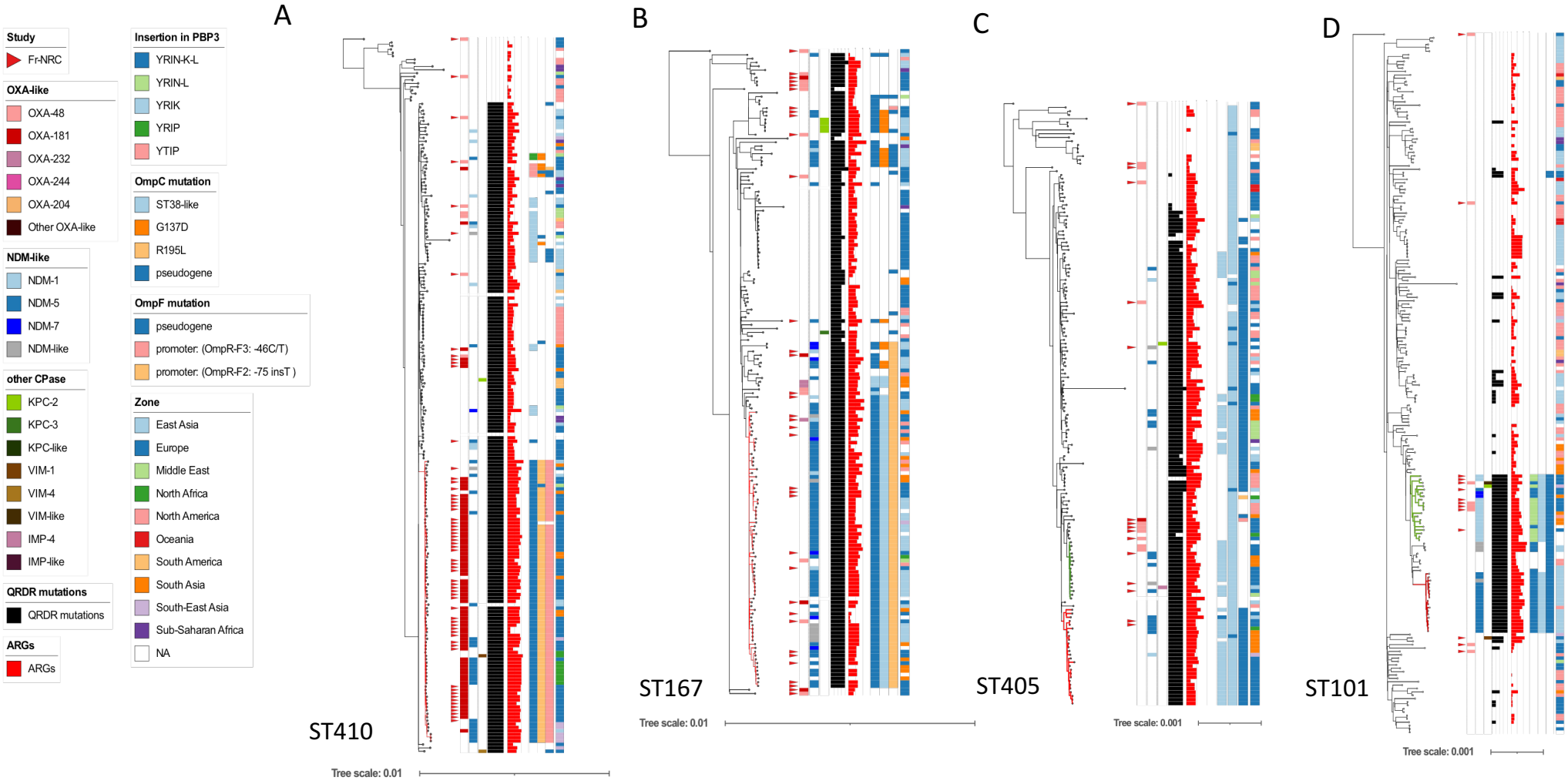

Figure S2. **Core genome phylogenies of the main ST characterized by clades disseminating internationally.** A. ST410; B. ST167; C. ST405; D. ST101. Phylogenies were based on genome sequences of A: 64 CP-*Ec* from the F-NRC and 146 genome sequences from the NCBI database;B: 35 CP-*Ec* from the F-NRC and 134 genome sequences from the NCBI database; C. 15 CP-*Ec* from the F-NRC and 145 genome sequences from the NCBI database; D. 13 CP-*Ec* from the F-NRC and 194 genome sequences from the NCBI database. Core genome (ST410: 3,522,000 nt; ST167: 3,276,000 nt; ST405: 3,685,000 nt; ST101: 3,774,000 nt) alignments of the *de novo* assemblies on the sequences of GCA_001442495.1 (ST410), GCA_003028815.1 (ST167), GCA_002142675.1 (ST405), GCA_002163655.1 (ST101) used as reference were performed by using Parsnp; ML phylogeny was built with RAxML from 6,176 (ST410), 10,393 (ST167), 37,482 (ST405), 19,967(ST101) core SNPs after removing recombined regions with Gubbins. The genome sequences of CNR93E7 (ST88), CNR93D10 (ST746), CNR73I9 (ST115), CNR93I2 (ST906) were used as outgroups for the phylogenetic analyses of ST410, ST167, ST405 and ST101 respectively. The origin from the F-NRC is indicated by red triangles close to the isolate name. Other genomic features are indicated as indicated in the figure key (left) from the inside to the outside lines: carbapenemases of the OXA, NDM and other types, number of mutations in *gyrA* and *parC* QRDR region (FQ resistance), number of ARGs, mutations in *ftsI*, *ompC*, *ompF*, geographical origin.

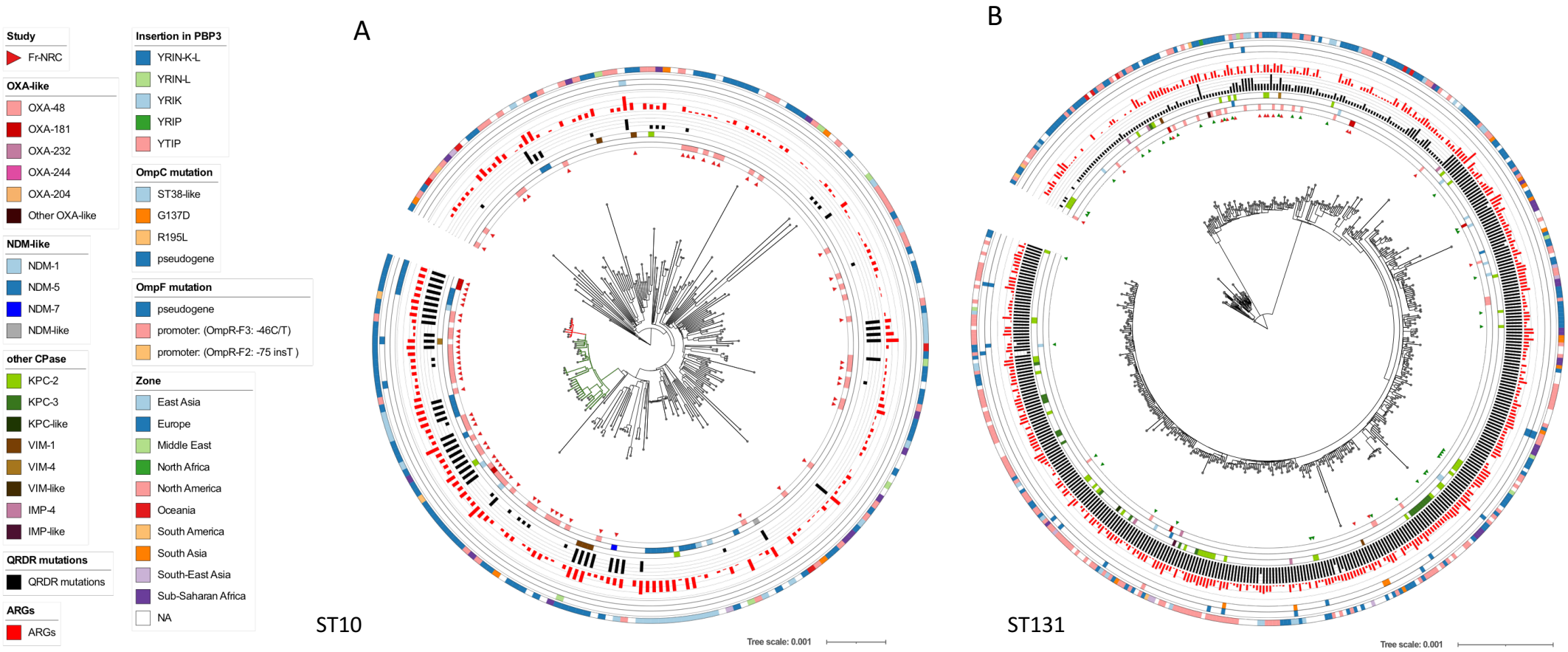

Figure S3. **Core genome phylogenies of ST10 and ST131 isolates. A.** ST10 phylogeny based on the genome sequences of 67 CP-*Ec* from the F-NRC and 153 genome sequences from the NCBI. **B.** ST131 phylogeny based on the genome sequences of 17 CP-*Ec* from the F-NRC and 462 genome sequences from the NCBI. Core genome (ST10: 813,000 nt; ST131: 1,641,000 nt) alignments of the *de novo* assemblies on the sequence of MG1655 (ST10) or GCA_000285655.3 (ST131) used as references were performed by using Parsnp; ML phylogeny was built with RAxML from 20,245 (ST10) and 14,366 (ST131) core SNPs after removing recombined regions with Gubbins. The genome sequences of CNR93D10 (ST746) and CNRAL47G10 (ST640) were used as outgroups for the phylogenetic analyses of ST10 and ST131, respectively. F-NRC isolates are indicated by red triangles (inner circle). Other genomic features are indicated as indicated in the figure key (left) from the inside to the outside circles: carbapenemases of the OXA, NDM and other types, number of mutations in *gyrA* and *parC* QRDR region (FQ resistance), number of ARGs, mutations in *ftsI*, *ompC*, *ompF*, geographical origin. The ST10 clade enriched in CP-*Ec* is indicated in green and the sub-clade with the YRIN insertion in PBP3 in red. Note that the circle for *ftsI* mutations is absent in ST131, as no YRIN-like duplication in PBP3 was identified among the analyzed isolates.

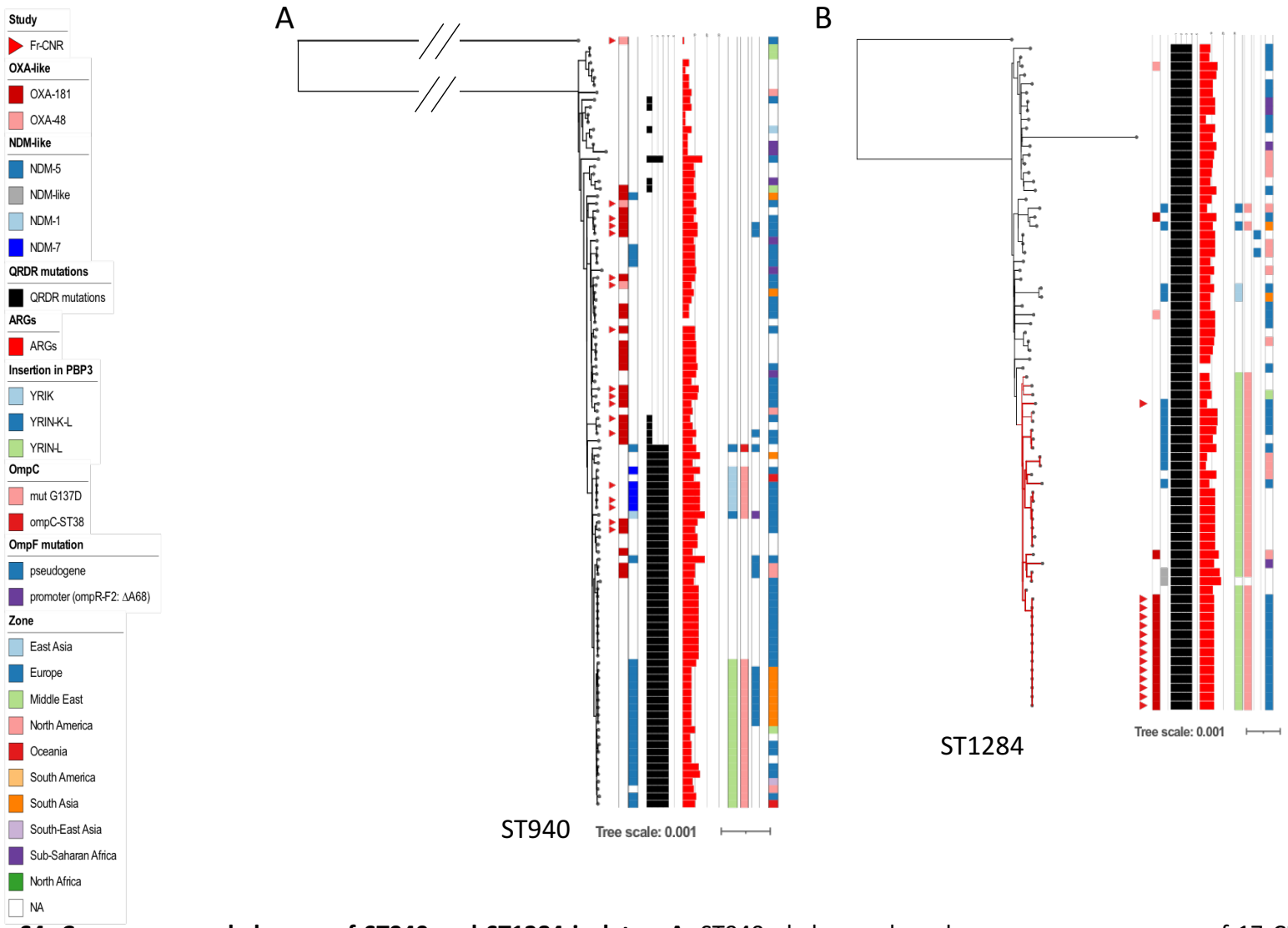

Figure S4. Core genome phylogeny of ST940 and ST1284 isolates. A: ST940 phylogeny based on genome sequences of 17 CP-*Ec* from the F-NRC and 88 genome sequences from Enterobase and the NCBIdatabase **B:** ST1284 phylogeny based on genome sequences of 14 CP-*Ec* from the F-NRC and 60 genome sequences from Enterobase and the NCBI database. A core genome (ST940: 3,639,000 nt; ST1284: 3,779,000 nt) alignment of the *de novo* assemblies on the sequence of ST940: ESC_LB2149 and ST1284: ESC_LB2152AA (from Enterobase) used as references was performed by using Parsnp; ML phylogeny was built with RAxML from 13,859 (ST940) and 2,009 (ST1284) core SNPs after removing recombined regions with Gubbins. The genome sequences of CNR98G1 (ST3022) and MG1655 (ST10) were used as outgroups for the phylogenetic analyses of ST940 and ST1284, respectively. F-NRC isolates are indicated by red triangles first column on the left. Other genomic features are as indicated in the figure key (left) from the left to the right columns: carbapenemases of the OXA, NDM and other types, number of mutations in *gyrA* and *parC* QRDR (FQ resistance), number of ARGs, mutations in *ftsI*, *ompC*, *ompF*, geographical origin.

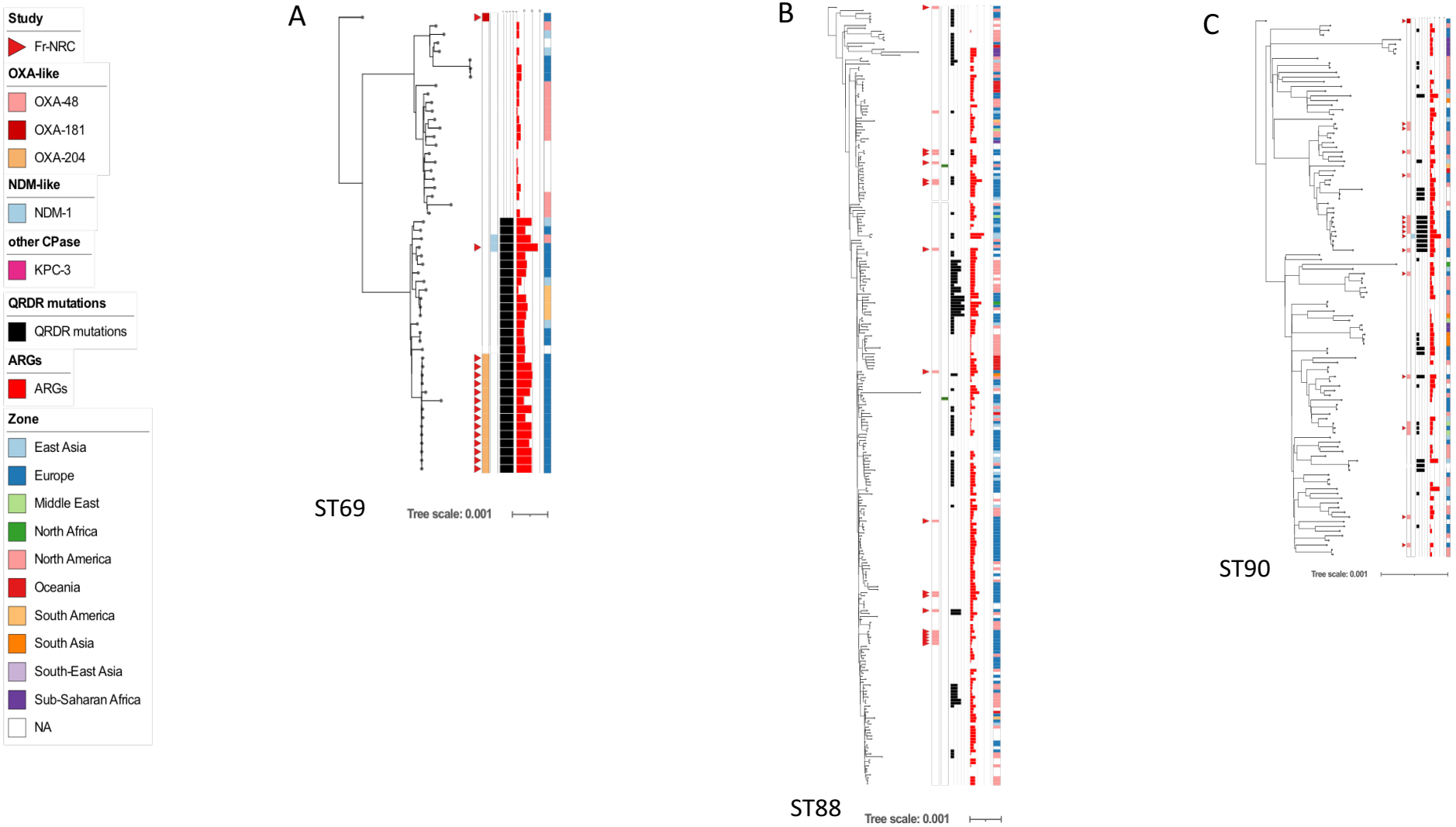

Figure S5. **Core genome phylogenies of ST69, ST88 and ST90. isolates. A:** ST90 phylogeny based on the 15 CP-*Ec* from the F-NRC and 38 genome sequences from the NCBI database**; B:** ST69 phylogeny based on the 16 CP-*Ec* from the F-NRC and 244 genome sequences from the NCBI database; **C.** ST88 phylogeny based on the 15 CP-*Ec* from the F-NRC and 99 genome sequences from the NCBI database. Core genome (ST69: 2,735,000 nt; ST88: 3,472,000 nt; ST90: 3,801,000nt) alignments of the *de novo* assemblies on the sequence of GCA_002443135.1 (ST69), GCA_002812685.1 (ST88) or GCA_001900635.1 (ST90) used as references were performed by using Parsnp; ML phylogeny was built with RAxML from 4,596 (ST69), 12,557 (ST88) or 2,878 (ST90) core SNPs after removing recombined regions with Gubbins. The genome sequences of CNR33D9 (ST394), CNR83B9 (ST410) and CNR88B9 (ST847) were used as outgroups for the phylogenetic analyses of ST69, ST88 and ST90, respectively. F-NRC isolates are indicated by red triangles (first column on the left). Other genomic features are indicated as indicated in the figure key (left) from the left to the right columns: carbapenemases of the OXA, NDM and other types, number of mutations in *gyrA* and *parC* QRDR (FQ resistance), number of ARGs, mutations in *ftsI*, *ompC*, *ompF*, geographical origin.

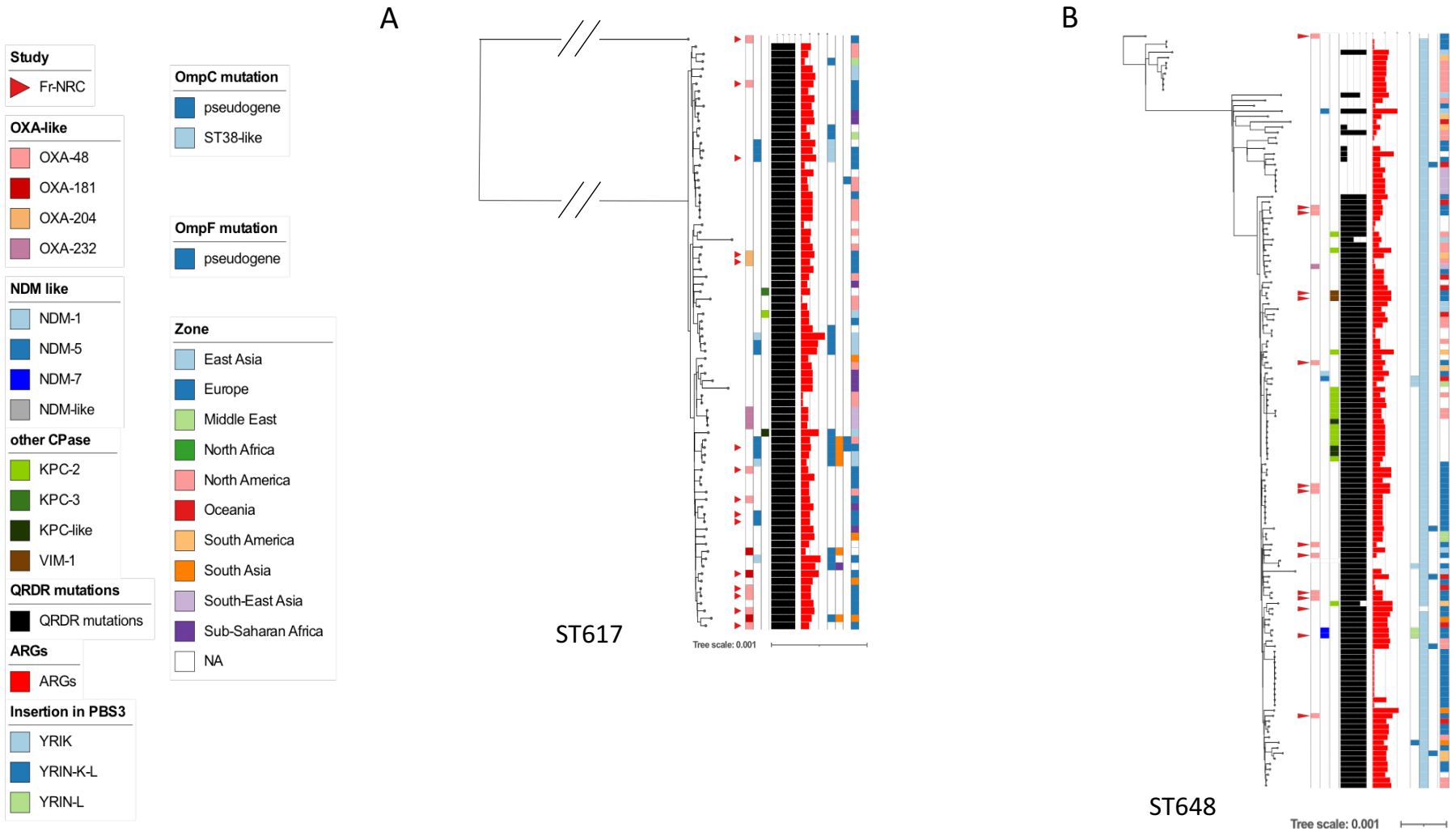

Figure S6. **Core genome phylogeny of ST617 and ST648 isolates A**: ST617 genome sequences of 15 CP-*Ec* from the F-NRC and 65 genome sequences from the NCBI database; **B**: ST648 genome sequences of 14 CP-*Ec* from the F-NRC and 126 genome sequences from the NCBI database. A core genome (ST617: 3,407,000; ST648: 3,501,000 nt) alignment of the *de novo* assemblies on the sequences of GCA_002142695.1 (ST617) or GCA_004138645.1 (ST648) used as references was performed by using Parsnp; ML phylogeny was built with RAxML from 15,030 (ST617) or 3,782 (ST648) core SNPs after removing recombined regions with Gubbins. The genome sequences of CNR93D10 (ST746) and CNR71A8 (ST1485) were used as outgroups for the phylogenetic analyses of ST617 and ST648, respectively. F-NRC isolates are indicated by red triangles close to the isolate name. Other genomic features are indicated as indicated in the figure key (left) from the left to the right columns: carbapenemases of the OXA, NDM and other types, number of mutations in *gyrA* and *parC* QRDR (FQ resistance), number of ARGs, mutations in *ftsI*, *ompC*, *ompF*, geographical origin.